CHAPTER 1.3

Automated Mineralogy

Mark G. Aylmore

Automated mineralogy is a term that has been used to describe the automation of the analytical process of quantifying minerals, rocks, and production materials. Analytical techniques, such as X-ray powder diffraction and optical and electron microscopy, have been extensively used over the years to describe the mineralogy in geological and metallurgy applications (Petruk 1976; Petruk and Hughson 1977; Cabri 1981; Petruk and Schnarr 1981; Henley 1983; Petruk 2000; Gu, 2003).

With advances in computing power and speed, automated mineralogy techniques have been developed for the minerals industry and used in research institutes for more than two decades. This has primarily been in the areas of X-ray analysis and commercialized in the form of scanning electron microscope (SEM) techniques such as mineral liberation analysis (MLA) and Quantitative Evaluation of Minerals by Scanning Electron Microscopy (QEMSCAN); and more recently, Tescan Integrated Mineral Analyzer (TIMA), Zeiss Mineralogic, INCAMineral (from Oxford Instruments), and Advanced Mineral Identification and Characterization System (AMICS), developed by Yingsheng Technology and now marketed through Bruker Inc. As a result of the improvement in technology, automated mineralogy systems are now regarded as essential by most large companies and used on a routine basis to supply metallurgical operations with regular data (e.g., Barrick Gold, Kennecott Utah Copper Corporation [KUCC], Anglo American, Freeport-McMoRan, Richards Bay Minerals, and Northparkes). There are more than 150 automated SEM systems in operation worldwide (Schouwstra and Smit 2011).

Comprehensive and rapid analysis techniques play an important role in geometallurgy evaluations, such as for scoping; prefeasibility and feasibility studies; process design; and optimization of gold, copper gold, copper molybdenum, nickel, and iron projects (Williams and Richardson 2004; Dobby et al. 2004; Bulled 2007; Bulled et al. 2009; Lotter et al. 2013; Kormos et al. 2013; Montoya et al. 2011; Hatton and Hatfield 2013; Baumgartner et al. 2011, 2013; Hoal et al. 2013; Zhou and Gu 2016).

The application of automated mineralogical techniques can have the following benefits:

- Reduce and circumvent risks associated with the variability of ore bodies during project evaluation, process development, plant design, mine planning, and performance of mineral processing/metallurgical unit operations.
- Provide ongoing ore characterization analysis tools to track and reduce costs in mining, processing, and tailings handling.
- Coupled with other diagnostic sampling techniques used in a plant, automated mineralogy systems can improve the statistical reliability of mineralogical and process measurements for plant surveys (Henley 1983; Lotter 1995, 2011).
- De-bottlenecking of existing or recent design and plant restarts can be executed faster and more cost efficiently with process mineralogical support (Baum 2014).
- Automated central laboratories or smaller mine site laboratories can provide efficient, better quality, and fast laboratory data for exploration and mine geology samples, geometallurgy programs, daily blastholes, and all other production samples (Best et al. 2007).
- Track the deportment of minerals or metals in process streams. Routine analyses to track precious metals associated with other minerals is more efficiently handled.
- Allow semiskilled personnel to operate and free mineralogical staff to perform research into improving and understanding ore and processing issues.

This chapter provides an overview of the main analytical techniques used in automated mineralogy routines that are available to metallurgists. The first two parts cover the main X-ray analysis and digital imaging techniques. The limitations and some applications illustrating these techniques are also described. Semiautomated microprobe techniques are described in the subsequent sections and are included, as they are commonly used to confirm and back up routine automated techniques. High-resolution X-ray computed tomography is briefly discussed at the end of this chapter.

Mark G. Aylmore, Senior Research Fellow, John de Laeter Centre, Faculty of Science & Engineering, Curtin University, Perth, Western Australia, Australia

To utilize the analytical techniques described in this chapter effectively, it is important that the metallurgist first define the type of information required, with consultation of experienced analysts before choosing an analytical method or strategy. All analytical techniques require some validation by other techniques and need to be tailored for the process and operation under consideration. For personnel to operate automated mineralogy techniques requires training and a basic understanding of physics concepts to maximize benefits.

X-RAY ANALYTICAL TECHNIQUES

The two most commonly used X-ray methods are X-ray powder diffraction (XRPD) and X-ray fluorescence (XRF) spectrometry. Although other techniques based on the scatter, emission, and absorption properties of X-radiation can be used in different scenarios, such as surface analysis, they are not discussed here.

X-Ray Powder Diffraction

XRPD is one of the most powerful techniques for qualitative and quantitative analysis of crystalline compounds and is widely used in most analytical laboratories for mineral or phase identification. The information that can be obtained includes

- Types and nature of crystalline phases present,
- Relative abundance of major mineral phases,
- Microstrain and crystallite size, and
- Isomorphic substitution trend mineral phases.

All these attributes can affect the reactivity of minerals in metallurgical processes.

Instrumentation

A typical X-ray powder diffractometer setup with sample changer is shown in Figure 1. Bragg-Brentano focusing geometry is the most widespread geometry used in XRPD methods in both research and industrial laboratories (Klug and Alexander 1974). The geometry of an X-ray diffractometer is such that the sample rotates in the path of the collimated X-ray beam at an angle θ while the X-ray detector is mounted on an arm to collect the diffracted X-rays and rotates at an angle of 2θ. Copper anode is the most common and cheapest target material used in most applications for generating an X-ray source. However, copper anode with a post-sample graphite monochromator or cobalt anodes are frequently used in samples that contain high cobalt, iron, and manganese content, where fluorescence in the X-rays produced from a copper target yield a low peak-to-background ratio in powder diffraction data. Solid-state strip detectors can replace point detectors in diffractometers, which allows a decrease in measurement scanning times from several hours to 10 minutes.

Most of the X-ray diffractometers from the major manufactures have the facilities to handle and collect data for multiple samples. In addition, there are several commercial-size machines developed specifically for industry, such as the Malvern Panalytical CubiX^3 and Bruker D4 Endeavor.

Information Provided from X-Ray Powder Diffraction

Details on the theory and fundamentals of XRPD are well documented, both on websites and in the literature (e.g., Zevin et al. 1995; Bish and Post 1989; Cullity 1978; Klug and Alexander 1974). X-ray diffraction (XRD) is based on constructive and destructive interference of monochromatic

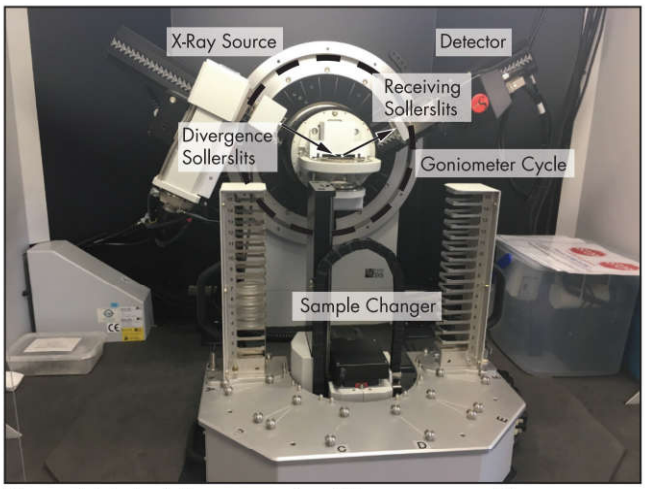

Figure 1 Typical X-ray powder diffractometer with conventional Bragg-Brentano focusing geometry

X-rays in a sample. Most (95%) solid materials are crystalline. The interaction of the incident X-rays with the sample may produce constructive interference and a diffracted X-ray when conditions satisfy Bragg's law ($n\lambda = 2d \sin \theta$, where n is an integer, λ is the wavelength of incident beam, d is the interplanar spacing, and θ is the scattering angle).

The position and intensity of peaks in a diffraction pattern are determined by the crystal structure. The unique set of d-spacings derived from a powder diffraction pattern can be used to *fingerprint* the mineral. Using software normally provided by the manufacturers of XRPDs, phases that are present in a sample can be compared with databases such as the Powder Diffraction File (PDF) produced by the International Centre for Diffraction Data (ICDD), which contains the d-spacing, intensity lists, crystal structures, and literature reference information for thousands of crystalline phases. An example of an XRPD pattern for a titanium-rich material with mineral phases identified from the ICDD-PDF database is shown in Figure 2. The minimum detectable limit found by routine qualitative procedures is of the order of ~1%, which restricts ore mineral quantification to concentrates and upgraded feed and tailings samples. Complete analysis requires several hours to complete, although this depends on the experience of the analyst and the complexity of the problem under investigation. For typical powder patterns, data can be collected over a short 2θ range from ~5° to 90° for qualitative analysis of most minerals; full 2θ range is required for full structural refinement applications.

The appropriate data-collection strategy will depend on the nature of the sample, for example, on how well it scatters, peak-broadening effects, and the degree of peak overlap (McCusker et al. 1999). Overall step size should be at least one-fifth of the full width at half-maximum of a diffraction peak, and time per step should approximately compensate for the gradual decline in intensity with 2θ (Madsen and Hill 1990, 1994). The types of information that can be extracted from XRPD are listed in Table 1.

Most industrial processes are interested in changes in the abundance of particular mineral phases and not always concerned with detailed mineral structural properties. However, depending on the analysis method used, it is important that sufficient detail is available for a mineral phase of interest to

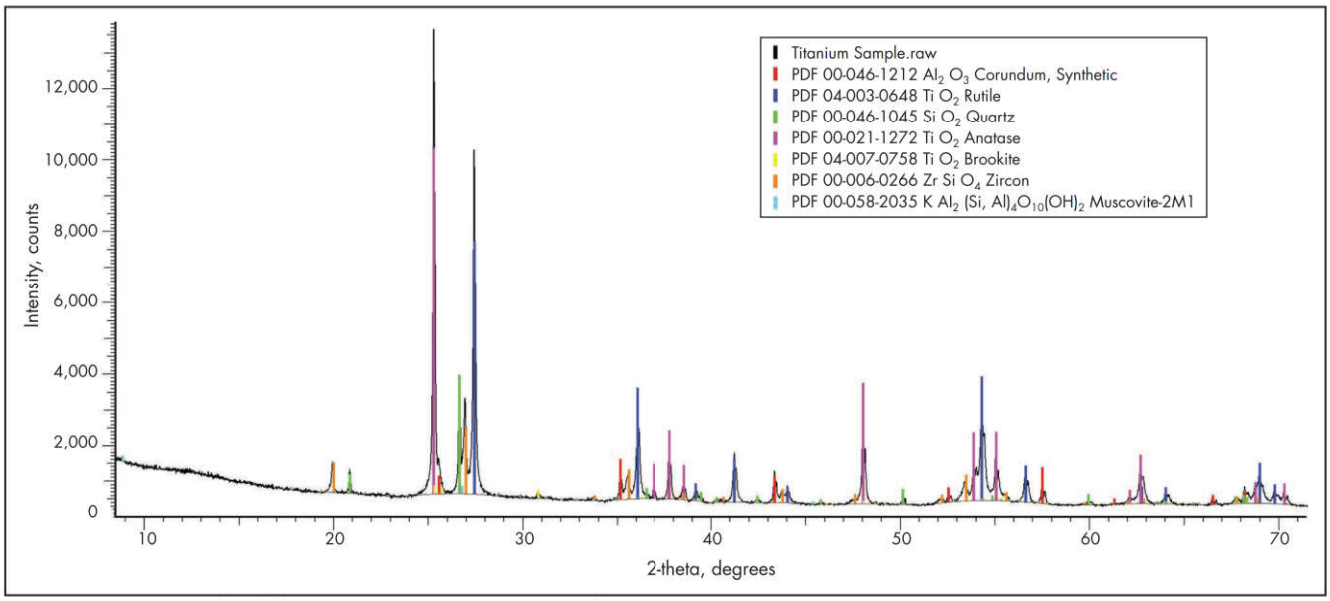

Figure 2 X-ray powder diffraction pattern (copper Ka radiation)

Table 1 X-ray powder diffraction pattern information

Peak Reflection Information					Background Fit
Position		Intensity		Profile, Width and Shape	Sample
Qualitative phase analysis	Lattice parameters	Quantitative phase analysis	Crystal structure	Sample broadening	Diffuse scattering
Identification of individual phase(s)	Composition Macrostrain Space group	Abundance of phases	Atomic positions Temperature factors Site occupation factors	Crystalline size Microstrain	Amorphous fraction

either model or use data from powder diffraction patterns to confidently ascertain the correct information. Furthermore, details on crystallite size, strain, *amorphous* content, and isomorphic substitution of elements within minerals (e.g., Al or Ni in goethite) are important for consideration in many metallurgical applications.

Sample Preparation

How samples are prepared affects the quality of the data collected. The issues and best practices for sample preparation are well documented (Hill and Madsen 2002; Buhrke et al. 1997; McCusker et al. 1999). The main sample issues that affect the powder diffraction data are as follows:

- **Sample not representative.** The sample is not homogenized during sample preparation.
- **Particle size.** Coarse-size particles yield insufficient diffracting particle statistics (i.e., low peak-to-background ratio).
- **Preferred orientation.** Particles lie in a preferred orientation, resulting in enhanced diffraction at the angle (Dollase 1986; Li et al. 1990; O'Connor et al. 1991).
- **Microabsorption effects.** For high X-ray absorbers (e.g., rutile), only a fraction of grains diffract, resulting in underestimation of relative intensity; whereas for low absorbers (e.g., corundum), the beam penetrates more grains, resulting in more diffracting volume and an overestimation of the relative intensity.
- **Extinction.** Reduction in the intensity is caused by rediffraction of a Bragg reflection toward the incident beam.
- **Sample transparency.** For materials with light elements, the X-rays penetrate too deeply into the sample, yielding shifts in peak positions and relative peak intensities.

Fortunately, many of these issues can be reduced by ensuring that samples are ground fine enough to irradiate or dilute these effects. In addition, a sample spinner is used to improve sampling statistics. Although there are methods for modeling and correcting these effects, good sample preparation and correct setup of instrumentation is essential. This reduces the need for corrections.

For small volumes of sample, an agate mortar and pestle can be effective, but micronizing is the most efficient method for generating particle sizes of ~10 μm with a small spread of sizes. For large sample volumes, there are several commercial units for automated sample preparation on the market. Overgrinding can cause merging of particles, solid-state phase transformations (e.g., calcite to aragonite, wurtzite to sphalerite, kaolinite to mullite), loss of crystallinity, peak broadening, or amorphization of phases in samples (Buhrke et al. 1997).

There are many different ways samples can be mounted for XRPD analysis. These include top loading and pressing, flat plate, back loading and pressing, and side drifting. Using back-pressing and side-drifting loading methods reduces the issues associated with preferred orientation compared with top-loading or front-mounted samples. Solid diluents (e.g., gum, glass, gelatin) or binders can be added to reduce

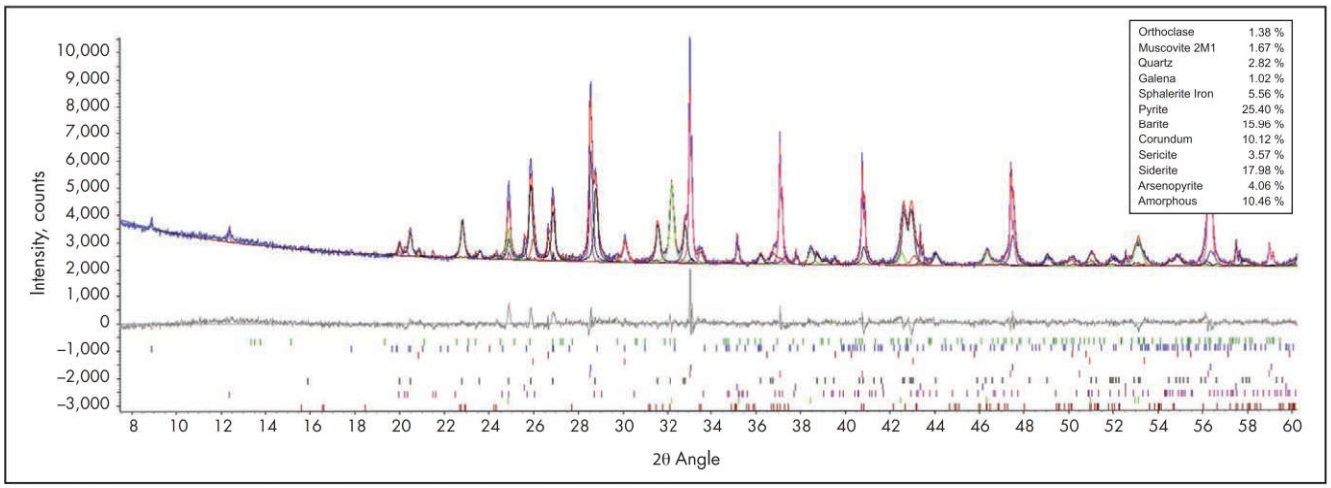

Figure 3 Output patterns for refinement of a zinc and lead sulfide ore

preferred orientation effects, but result in sample contamination, increased transparency issues, amorphous scatter, and/or extra peaks in powder diffraction patterns. For large-scale preparation operations, automated soft-pressing machines (e.g., FLSmidth ASP100) have been designed to prepare mounts for quantification by XRPD and other techniques (e.g., near-infrared spectroscopy, XRF) (Hem et al. 2009).

Some phases have crystal habits (platy or needle like), which promote orientation along specific crystallographic directions (e.g., micas, clay minerals, albite, sanidine, chlorite); therefore, preferred orientation issues cannot be eliminated. In some cases, the preferred orientation is deliberately enhanced for the identification of swelling clay minerals (Brindley 1980). The characterization of clay layers is carried out by XRD on air-dried and glycol-saturated oriented preparations on ceramic holders, sometimes after saturation with different cations (e.g., K, Mg, Li) (Bouchet et al. 1988). The addition of glycolation to the sample is used to identify the nature of the nonswelling clays (e.g., illite or chlorite); discriminate between the swelling clays (di- or trioctahedral high-charge or low-charge smectite, vermiculite); and quantify the nature, degree, and ordering of the mixed layering within phyllosilicate systems (Mosser-Ruck et al. 2005).

Quantitative Analysis

Detailed information on quantitative X-ray diffraction (QXRD) can be found in books such as Zevin et al. (1995) and the chapter by Madsen et al. (2012). Once the presence of phases has been established in a given specimen, the abundance of a phase or many phases present can be determined by use of the intensities of diffraction lines from each phase.

Rietveld and profile-fitting methods. Nowadays, the Rietveld method (Rietveld 1969; Young 1995) is the most employed methodology to achieve quantitative phase analysis (QPA) of crystalline materials (Snyder and Bish, 1989; Madsen et al. 2001; Scarlett et al. 2002; Hill and Howard 1987; Hill 1991; Bish and Post 1993; Hill et al. 1993). It allows an accurate estimation of changes in the mineralogical composition of solids or slurries. Detailed information on the theory of the Rietveld method can be found in Young (1995). The principle of the method is that the intensities calculated from a model of the crystalline structure are fitted to the observed X-ray powder pattern by a nonlinear least-squares refinement. The crystal-structural data (unit cell dimensions, space group, atomic positions, and thermal parameters) for each phase are obtained either within the software or sourced from the Inorganic Crystal Structure Database. To obtain high-quality quantitative results, the X-ray diffractometer is aligned and calibrated with a suitable standard (e.g., lanthanum hexaboride [LaB_6], National Institute of Standards and Technology standard reference material [SRM] 660a).

The refinement of crystal-structural and peak-profile parameters enable physical and chemical details of each particular phase in the mixture to be modified. In addition to phase abundance derived from the relative intensity of phases modeled in the XRPD pattern, the refinement of the lattice parameters of the phase can be used to calculate compositions in solid solution (e.g., Al substitution in goethite) and crystallite sizes determined from peak line broadening. Other crystal structure parameters, such as atomic coordinates, atomic site occupancies, and thermal parameters can be refined or modified in the initial setup and fixed for analysis of samples on a process production scale. The weighted profile R factor is monitored for convergence, often expressed as a percentage, and should be less than 10% for a good fit.

Most software packages provide a graphical representation of the calculated and measured XRD pattern and the difference plot to allow any misfit of data to be easily recognized. Figure 3 is an example of an output for the refinement of a zinc and lead sulfide ore, showing observed, calculated, and difference patterns. The hkl positions for each mineral are also give in order of the minerals listed.

Where all phases in the mixture are known, are crystalline, and have known crystal structures, the relative mineral abundances can be calculated from the Rietveld refined scale factor and a *phase constant* ZMV (Z is the number of formula units in the unit cell, M is the molecular mass of the formula unit, and V is the unit cell volume) for each phase (Hill and Howard 1987).

Where phases have a partial or no known crystal structure, there are methods that can be employed to quantify phases. Such an approach has been described by Scarlett and Madsen (2006) (partial or no known crystalline structure, or PONKCS method) and used in applications such as quantifying cement (Madsen and Scarlett 1999; Scarlett et al. 2001; Taylor and Rui 1992). In these methods ZM and V are empirical values

derived by preparing a mixture of the phase of interest with a known, well-characterized standard.

There are a few Rietveld-type software packages available for commercial use. One of the most popular is the TOPAS software, which has two modes of operation. A graphical user interface mode is available where all data entry is handled through parameter windows and is useful for routine operation in profile-fitting and Rietveld applications. The launch mode is designed for crystal structure solutions and for automation or batch operation applications. Data entry is through text files and allows advanced users to write their own functionality.

Approach to modeling and quantifying phases in samples. For analyzing and quantifying the mineralogy of a group of samples by XRPD, the following approach can be used:

- Preliminary setup
  - Identify minerals and grouping of sample XRPD data with similar mineralogy to facilitate defining mineral suites that can be modeled.
  - Ensure that XRPD instrumental parameters are defined to allow for accurate modeling of artifacts in XRPD scans associated with the XRPD instrument (e.g., detector aberrations, tungsten radiation peaks, unfiltered peaks).
  - In some cases, assess synthetic mineral mixtures of like minerals to improve confidence in the ability to model and quantify phases.
- Preparation of mineral templates for modeling XRD scan data
  - Compile structural data for each mineral phase identified in the sample.
  - Refine and fit profile to sample XRPD data.
  - Confirm fit with chemical assay data and/or synthetic mineral mixtures.
- Batch refinement on materials with similar compositions and areas (e.g., lithological zones)
- Correlation and cross checking of chemical data derived from mineral refinements with chemical assay data or other analysis methods such as a thermogravimetric analysis and digital image analysis techniques.

Amorphous content. In many naturally occurring or synthetic systems, poorly ordered phases may be present that cannot be accurately modeled by published structure information in the literature. The presence of poorly ordered phases will have an influence on the reactivity and dissolution of ores, such as dissolution of amorphous silica and polymerization in acid uranium extraction circuits, or may affect the flotation response of some minerals.

Amorphous phases cannot always be detected directly by XRD analysis, because they do not produce visible peaks in the XRD pattern, but only increase the background. There are several methods that can be used for determining amorphous content by XRPD (Madsen et al. 2011). The most common one is the internal method where the sample is *spiked* with a known mass of standard material (e.g., calcium fluoride [CaF_2], corundum). The weight fractions of the crystalline phases present in the sample are estimated using the Rietveld analysis. For a sample containing an amorphous phase, the standard will be overestimated in the analysis. From the overestimation of the standard, the amorphous content of the investigated sample is derived. However, the determination of amorphous content value is sensitive to how well the experimental and calculated data fit, as well as the assumption that all phases present in the sample have been identified and modeled.

Main Sources of Error and Limitations in Quantitative Analyses

Sources of errors have been identified in several round-robin surveys conducted by the International Union of Crystallography Commission on Powder Diffraction to evaluate QPA by powder diffraction (Madsen et al. 2001; Scarlett et al. 2002):

- In some cases a poor understanding of issues in data collection and analysis leading to Rietveld software to be treated as a *black box*
- Incorrect crystal structure data chosen or inappropriate profile models used
- Omission of phase(s) from the analysis and/or errors in identification of phases present
- Failure to refine important parameters such as unit cell and thermal values during modeling of phases
- Refinement of parameters not supported by the data
- Inappropriate use of correction models, such as preferred orientation and microabsorption correction
- Acceptance of physically unrealistic parameters (e.g., over refinement of thermal parameters) or incomplete refinements (high R factor values)

These issues can be overcome through continuing education of users of diffraction methodology and Rietveld-based software. The need for plant metallurgists to consult experienced XRPD analysts before placement of the analysis is emphasized by the surveys.

Problems still arise in the calculation of mineralogical phase abundance in cases where large extinction, preferred orientation, or microabsorption between different phases occur. The correction for these effects can be implemented in some Rietveld analysis programs (e.g., Madsen and Hill 1990; Taylor and Matulis 1991), but with caution. Microabsorption may not be avoided, but awareness of the effect gives an indication of over- and underestimation of phases. To improve precision and accuracy, it is useful to compare the results with alternative analysis methods (i.e., chemical analysis, automated SEM techniques). Precision can be determined through replicates. Calibration methods may also help for multiple samples of similar concentration and composition.

Applications

Rietveld-based QXRD has been extensively used for mineralogical characterization to understand the reaction chemistry and kinetics of mineral leaching and formation (e.g., Scarlett et al. 2008). The formation of new phases as a result of precipitation is often encountered during ore leaching processes, especially under high-temperature conditions, and the formation of these phases can be monitored by QXRD analysis (Whittington et al. 2003; Madsen et al. 2005). Some examples of the applications of Rietveld-based QXRD are illustrated in the following.

Bauxite Materials

The application of the Rietveld method to quantify minerals in bauxites has been reported by various workers (e.g., Aylmore and Walker 1998). A typical Rietveld refinement plot output from the assessment of a suite of bauxite samples from the

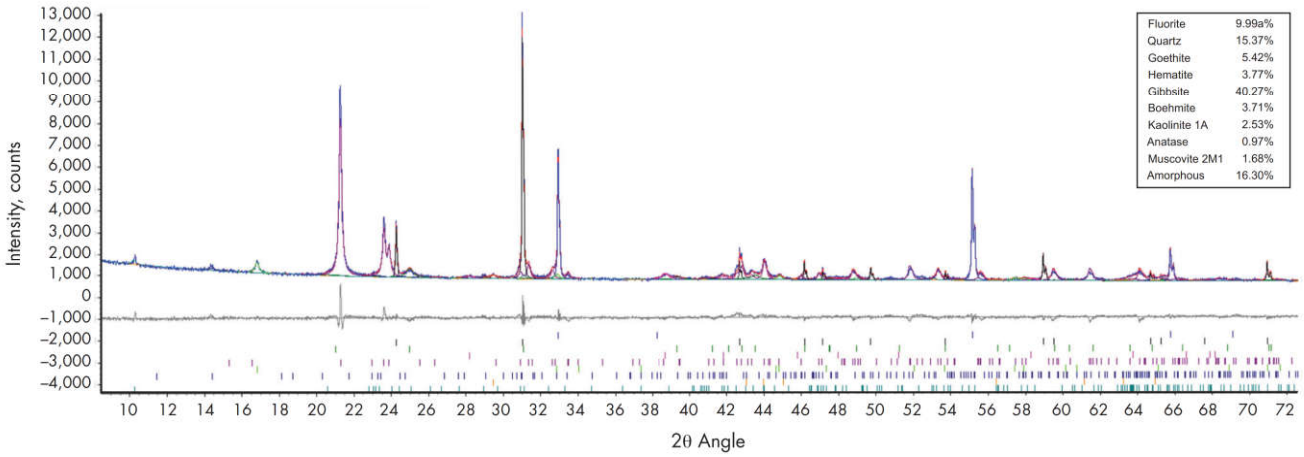

A. Typical output for Darling Range bauxite

Bauxite Sample	Gibbsite	Quartz	Goethite	Hematite	Boehmite	Kaolinite	Muscovite	Anatase	Maghemite	Al Substitution in Hematite	Al Substitution in Goethite
	wt %*									mol % (±0.6 mol %)	
1	47.7 (8)	21.9 (5)	16.1 (6)	6.7 (5)	—	1.0 (3)	4.5 (6)	1.8 (3)	—	8.4	27.7
2	55.1 (8)	21.0 (5)	7.5 (6)	5.1 (5)	5.0 (5)	2.3 (5)	2.3 (5)	1.3 (3)	—	16.5	30.4
3	42.4 (9)	15.5 (5)	22.1 (6)	8.5 (5)	4.8 (6)	—	2.4 (6)	1.6 (3)	—	9.5	28.5
4	46.8 (9)	22.9 (6)	10.2 (6)	6.4 (5)	5.4 (6)	1.5 (4)	2.5 (6)	1.1 (2)	1.6 (2)	10.1	33.3
5	56.2 (8)	23.8 (5)	9.8 (6)	2.6 (6)	3.2 (6)	2.4 (5)	1.5 (6)	1.1 (2)	—	9.9	32.8
6	59.5 (9)	1.9 (3)	19.5 (6)	9.7 (6)	2.6 (6)	2.5 (5)	—	6.6 (3)	—	5.3	9.3
7	69.6 (9)	0.5 (2)	15.7 (6)	6.4 (5)	1.9 (2)	1.5 (4)	—	5.6 (3)	—	8.6	20.6

*Estimated standard deviation of the least significant figure is shown in parentheses. Calcium fluoride (CaF_2) is used as internal standard to calculate amorphous content.

B. Rietveld analysis with calculated Al substitution values for hematite and goethite

Figure 4 (A) Rietveld refinement plot and (B) mineral abundance in bauxites

Darling Range in Western Australia and Rietveld-derived mineral abundance is shown in Figure 4. Observed, calculated, and difference patterns, together with hkl positions for each mineral, are shown in the figure. Refinement of the unit cell parameters enabled the level of Al substitution for Fe in structures to be calculated from the diffraction peak profiles of goethite and hematite. Variations in unit cell dimensions for goethite and hematite associated with Al substitution in the structures are well established for these minerals found in soils and bauxites (Fitzpatrick and Schwertmann 1982; Schulze 1984; Anand et al. 1989). The adjustment of site occupancy values in the structure files for goethite and hematite to reflect the substitution improved the correlation between predicted and calculated values for each mineral.

Poorly ordered phases cannot be accurately modeled by published structure information in the literature. However, if there is sufficient knowledge about the parameters that cause stacking faults, twins, or other extended imperfections within a phase, then it can potentially be modeled and quantified (e.g., kaolinite; Bookin et al. 1989; Neder et al. 1999). However, this type of work requires a specialist with crystallography knowledge to set up a model that can then be used by a metallurgist.

Investigating Reaction Pathways in Pressure Oxidation of Nickel Laterite and Sulfide Materials

Rietveld-based QXRD analysis can be applied to investigate reaction pathways and specifically the oxidation of sulfide minerals (e.g., Madsen and Scarlett 2007; Madsen et al. 2005; Whittington et al. 2003). Some good examples are illustrated by the work of Li et al. (2014) where the hydrothermal conversions of pyrrhotite and pentlandite were demonstrated and quantified using Rietveld-based QXRD analysis during the pressure oxidation of a nickel laterite concentrate. In this work, an intermediate nickel sulfide mineral phase with a cubic structure similar to vaesite and bravoite was identified. In another study, Rietveld-based QXRD analysis showed the co-processing of nickel laterite and sulfide inhibits the formation of basic ferric sulfate normally formed when treating sulfides in pressure oxidation. Quantitative XRD analysis was also applied to monitor the solid formation in the bioprocessing of iron-containing leach liquors and to characterize the mineralogy and crystallinity of the precipitates.

Cement Analysis

The Rietveld method has been successfully employed in industrial applications for QPA in complex hydrated systems such

as in the cement industry. The precision of quantifying clinker in laboratory and industrial approaches has been extensively evaluated in the cement industry (Walenta and Füllmann 2004), where precise and reproducible analysis of cement constituents of sulfate phases of gypsum, hemihydrate, and anhydrite, as well as calcite and portlandite are required. XRD studies were used to characterize the hydration reactions of mixed systems containing portland cements and calcium aluminate cements qualitatively. An online XRD instrument for continuously monitoring phase abundances was constructed and installed in an operational portland cement manufacturing plant (Scarlett et al. 2001). XRD data were simultaneously collected using a wide-range (120° 2q), position-sensitive detector to allow rapid collection of the full diffraction pattern. The data were then analyzed using a Rietveld analysis method to obtain a quantitative estimate of each of the phases present with high precision.

Elemental Analysis by X-Ray Fluorescence

XRF spectrometry is a well-established technique that can routinely measure elements from Na through U to complement the mineralogy measured by XRPD and other techniques. XRF is used for both qualitative and quantitative analysis of elements at low concentrations (sub–parts per million) in a wide range of samples to higher concentrations in limited quantities of materials.

A wide range of commercial instruments are available, which include benchtop models, handheld devices, and online process monitors. A schematic diagram of an XRF spectrometer is shown in Figure 5. XRF uses an X-ray tube similar to XRPD, providing an X-ray source, except that end window tubes are used (rather than side window tubes) for higher efficiency. Rhodium (Rh) is used as the standard anode material, as the characteristic energies of this element are simultaneously suitable for exciting both heavy and light elements. Some instruments are also equipped with a vacuum system for improving sensitivity for low-atomic-number elements.

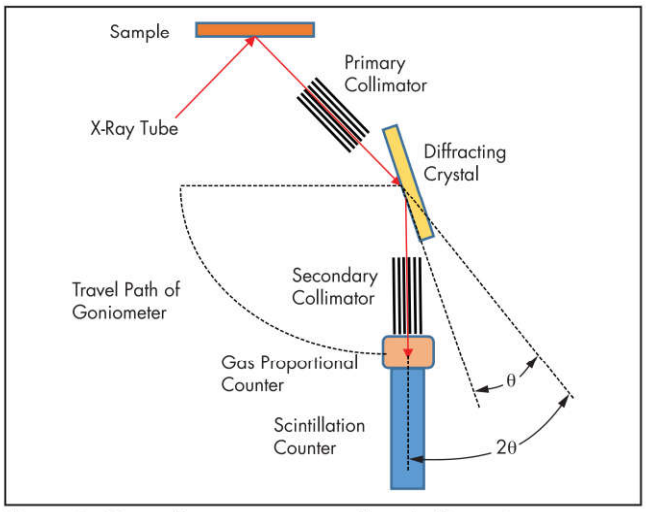

Figure 5 X-ray fluorescence wavelength dispersive spectrometry

Two kinds of instruments are used:

1. **Energy-dispersive X-ray (EDX) detection systems.** With energy ranges from 0.1 to 120 keV, these typically are benchtop size down to handheld models. They are usually employed for dedicated material-specific applications and general monitoring.
2. **Wavelength dispersive X-ray (WDX) systems.** These are widely used for more accurate, fast, and precise process and quality control applications in industry with 0.1–10 nm energy ranges.

EDX spectrometers tend to be more popular than WDX spectrometers because of their lower cost and ability to capture and simultaneously display information for various elements. However, they are more prone to spectral interference and are less accurate than WDX systems. EDX systems are better suited for the analysis of the transition elements and high-atomic-number elements.

Sample Preparation

The method of sample preparation for XRF analysis is dependent on the elements of interest, level of accuracy and precision required, detection limits, and turnaround time for analysis. For high-quality analyses of major and minor elements, fusion of the sample into glass disks with a meta- or tetraborate flux is used (Norrish and Hutton 1969). Sample preparation for the analysis of trace elements is usually accomplished by pressing powder briquettes, where the sample is mixed with a binder and subjected to elevated pressure. This method avoids the unnecessary dilution of the trace elements caused by a fluxing agent. Major element analyses can be carried out by this method, but samples have to be finely milled to reduce the absorption effect caused by coarse particles.

XRF analysis on slurries or loose powders can be done using online measurement instrumentation. However, the levels of precision and accuracy are compromised when compared to those obtained on fusion disk and powder briquette prepared samples.

Data Analysis

XRF analysis is prone to interference effects, but can be successfully addressed and corrected for utilizing computer-based algorithms (Rousseau 2006). The sensitivity of the spectrometer significantly varies, and the background varies by about two orders of magnitude over the wavelength range of the spectrometer. The sensitivity of the X-ray spectrometer decreases abruptly toward the long wavelength limit of the spectrometer mainly because of low fluorescence yields and the increased influence of absorption. Hence, the elements with lower atomic numbers at the long wavelength end of the spectrometer yield poorer detection limits (e.g., F, Na ~0.01% rather than parts per million; C, O the order of 3%–5%).

Reference spectra of thin film standards or pure element material are acquired, and individual elemental spectra are stored. These reference spectra are used in the standard deconvolution and mathematical separation of overlapping peaks of the unknown spectra. Spectral interferences (e.g., elemental peak overlap, escape peak, and sum peak interferences) are analyzed and attenuation corrections made.

DIGITAL IMAGING ANALYSIS TECHNIQUES

Digital imaging analysis involving microscopy techniques can provide the following information:

- Modal mineralogy
- Mineral associations
- Size-by-size liberation analysis
- Digital textural mineral maps
- Bright-field search for precious metal
- Grain size and shape
- Porosity

The advantages of automated digital image analysis techniques for mineralogical investigations over traditional microscopy techniques include fast acquisition time that provides a more statistically representative analysis of a sample as well as the ability to distinguish fine-grained or complex intergrown minerals at the micrometer scale. It also reduces the potential for operator bias and human error.

Optical Microscopy

Before performing any detailed quantitative analysis using automated mineralogy systems with SEM, it is good practice to examine samples with a standard optical microscope at the plant and/or at the analysis laboratory (Pirard 2016). Direct observation of specimens at low to intermediate magnification can provide information about microstructural defects, such as cracks, fissures, cleavages, pores, and grain boundaries, which can be overlooked when observing materials at the micrometer scale. In addition, some minerals are more readily identified by color and habit (e.g., flaky structure), which are not distinguished by backscatter imaging or X-ray analysis used in electron microscopy techniques. Optical microscopy can be carried out by either reflected light microscopy, which is suited for the imaging of most ore minerals, or transmitted light microscopy, which is more suited for the imaging of silicate gangue minerals.

Sample preparation can be similar or a precursor to electron microscopy techniques and does not require carbon coatings. Manual point counting techniques have traditionally been carried out on optical microscopes, but can be automated with camera-mounted systems to allow for digital process applications such as modal analysis. Optical microscopy resolution is not as good as that of SEM systems and does not distinguish minerals with variation in stoichiometries. In general, a larger number of measurements can be readily made by the automated SEM methods than can be attained with optical microscopy.

Electron Microscopy

In addition to the original commercial QEMSCAN and MLA systems now owned by Thermo Fisher Scientific, more recent developments include TIMA, Mineralogic, INCAMineral, and AMICS.

Instrumentation

Automated SEM systems consist of the following:

- The platform is SEM hardware.
- A backscatter electron (BSE) detector is standard with SEM equipment.
- One to four EDX spectroscopy detectors are mounted on the SEM. Most digital imaging analysis systems now use much faster liquid nitrogen–free Si drift detectors.
- User friendly operating and processing software with simplified or ready-made data outputs provide information on mineral speciation, composition, liberation, association, and size distribution.

Details on the theory and fundamentals of electron microscopy can be found on websites and in the literature (e.g., Amelinckx et al. 1997). The electron source in SEM can be a conventional tungsten filament; however, the latest generation of microscopes uses a field emission gun (FEG), which provides a more stable source, longer life span, and smaller spot size for improved BSE image resolution.

Automated SEM systems use a combination of backscatter imaging and X-ray analysis only for mineral identification and properties studies. Secondary electrons that provide images of the surface topography and other interactions (e.g., cathodoluminescence with appropriate detector) are not utilized in this process, although data can be collected simultaneously during analysis.

Backscattered electrons, which are elastically scattered electrons with energies close to the primary electron beam energy generated from tens of nanometers at the surface, are used for imaging compositional variations between phases. Minerals composed of heavier elements (e.g., zircon) backscatter more of the incident electrons of the SEM and appear

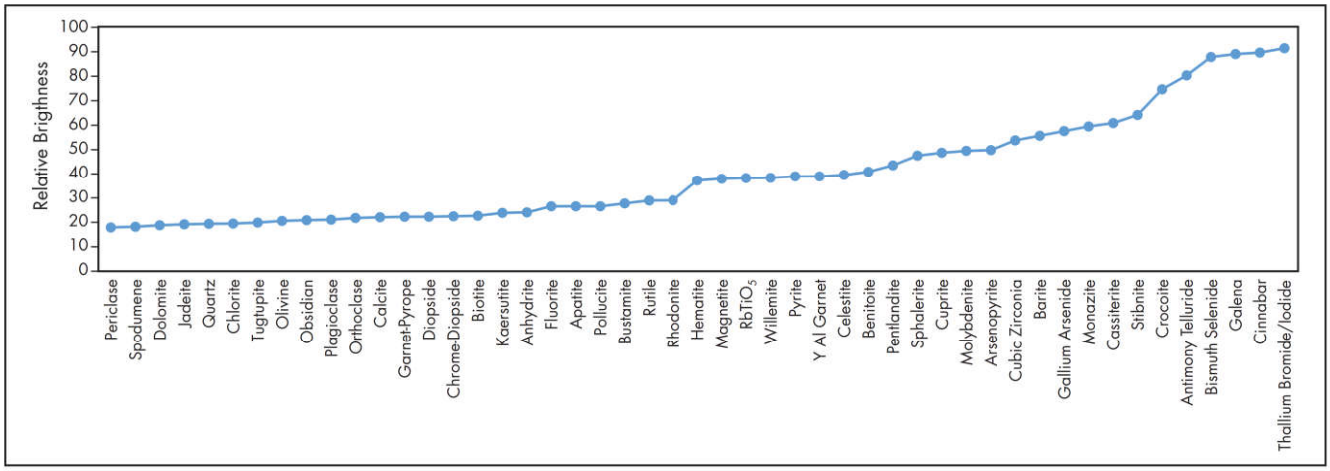

Figure 6 Relative backscatter electron intensity comparison

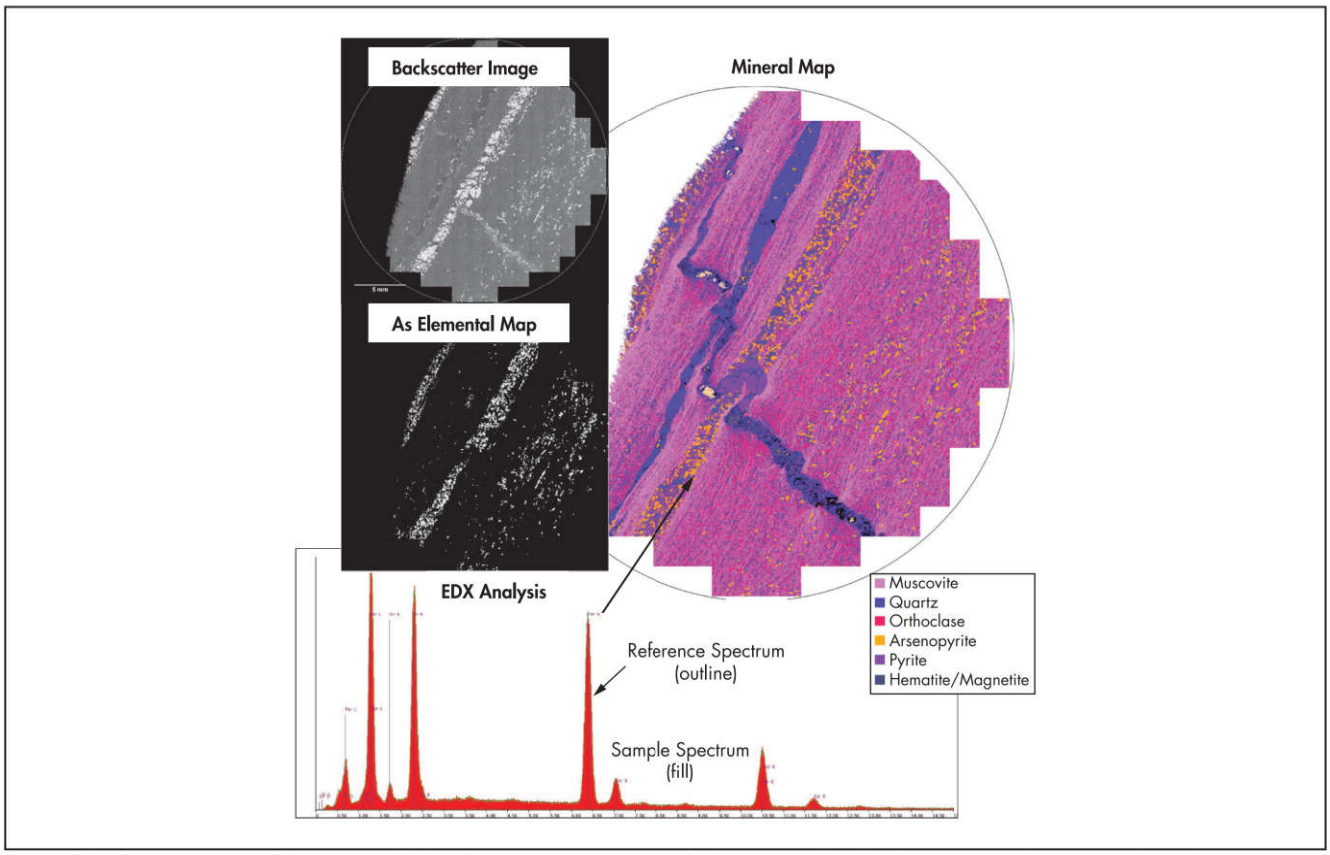

Figure 7 Mineral composition map with backscatter image, arsenic elemental distribution map, and energy-dispersive spectrum

brighter in the BSE image, whereas minerals composed of lighter elements (e.g., quartz) backscatter fewer electrons and appear darker. Figure 6 shows the relative intensities of some common minerals and phases.

The intensity variations (gray level) for different mineral phases in the BSE images provide an effective method of distinguishing the boundaries between mineral grains while the relative intensity values themselves provide a first-order identification of the minerals.

X-rays are produced by inelastic collisions of the incident electrons with electrons in the inner shells of atoms in the sample and are used to obtain the chemical composition of phases. Mineral classification by X-ray analysis is based on matching the entire spectrum of energy peaks collected on an unknown mineral to a library of X-ray spectra of known reference minerals collected using the same instrument parameters. From a combination of BSE contrast and matching EDX spectrum data files, mineral composition maps such as that shown in Figure 7 can be generated for the whole sample mount. The mineral maps can be used to describe the texture and mineral associations in each of the samples. As shown in the figure, the backscatter image depicts the contrast between sulfide minerals (light) and silicates (gray). The As elemental map illustrates the distribution of arsenic within grains in the polished mount and EDX analysis shows the arsenopyrite reference spectrum matching the sample grain spectrum.

The information is largely presented as two-dimensional (2-D) surface information with three-dimensional (3-D) electron beam interactions. Hence, grain boundaries and composition of mineral grains generated from X-ray data include interactions from 1 to 3 μm below the surface, depending on the beam conditions used. The size and shape of the electron beam surface interaction volume depends on the atomic number of the material being examined (a higher atomic number absorbs more electrons) and accelerating voltage being used (higher voltage results in deeper penetration and larger interaction volume).

Sample Selection and Preparation

As with any analytical technique, sample preparation is crucial to obtain reliable information. Samples analyzed can be large hand- or drill-core specimens, rock chips from percussion drilling or crushing circuits, or processed slurried samples from flotation and leach circuits. Some microscopes and software can accommodate polished blocks of different sizes.

Metallurgical plant samples are usually sized using dry and wet screening to eliminate agglomerated fine particles formed from previous filtering and dry procedures. To minimize biases associated with nonrepresentative sampling, riffling and subsampling prior to mounting are important. The selected samples for analysis are usually mounted in epoxy resin of 25- or 30-mm-diameter blocks or normal glass slides. In some cases, square blocks are used to maximize the area available for analysis.

It is important that the resin used for mounting has backscattering electron intensity less than the minerals or phases being measured to avoid misclassification with the background. In cases where carbon components are being measured, such

as coal or graphite, mounts can be prepared with the addition of carnauba wax and/or mounted in polyester resin (Liu et al. 2005; O'Brien et al. 2011). Polished sample mounts require a thin layer of carbon (25–50 nm) using a carbon evaporator or carbon coater to prevent charging during the analysis. The carbon-coated polished mounts are then loaded onto the multisample stage and placed in the SEM for analysis.

The main issues that affect the quality of the data that have to be taken into account when preparing polished mounts are as follows:

- The number of coarse particles (>500 μm) that can be mounted in a polished section are low and can lead to issues associated with statistical analysis representative of the size population. Hence, many polished mounts or mounts with a large surface area are analyzed.
- Very fine particles <~15 μm pose practical problems for mounting because of possible bias caused by particle loss during sieving and polishing and tend to agglomerate during the sample preparation. Generally, very fine-particle sizes are not measured and rely on other techniques such as XRPD to measure the mineral composition data or can be inferred to some extent from data at a coarser fraction size.
- Variation occurs in the specific gravity of mineral and phase components within a sample. Samples require careful sample preparation to prevent segregation of heavy particles from lighter gangue occurring within the section yielding a biased distribution. The process of double mounting to get representative samples can be used (Zhou and Gu 2016).
- The measurements of the size and shape of elongated particles can be biased by variable orientations. The use of a low-viscosity resin can allow preferential settling of particles with their largest face parallel to the surface of the mount (Tsikouras et al. 2011).
- For studies of minor to trace heavy minerals in rock or metallurgical samples, the sample should be concentrated to increase the number of heavy mineral grains available prior to mounting and analysis. In particular, the dense nature and low concentration of gold found in ores requires careful sample preparation to monitor.

Sample preparation can be the bottleneck when considerable volumes of samples are required to be processed. Batch productions of polished sectioned mounts are available (e.g., Struers Hexamatic). Automated sample loading and analysis are now available for batch analyses in some SEM systems.

Although surfaces should be polished for best analysis, the geometry of several detectors mounted around the microscope can allow for analysis of unprepared surfaces.

Collection and Analysis of Data

Different methodologies and philosophies have been used and developed over the years for collecting and analyzing data. The general concepts are discussed in the following sections.

Data Collection

In automated SEM systems, the voltage of the electron beam energy typically used is 25 kV, but lower energies can be used to reduce the interaction volume and improve imaging resolution. At 25 kV in a TIMA with FEG, the probe current is 5.78 nA and produces a spot size of 39.5 nm at a working distance of 15 mm. The automated software controls the SEM to collect BSE images and X-ray data by stepping across the polished mount or thin section by a series of fields in an equally spaced regular rectangular mesh.

Measurements are taken in each field based on chosen analysis type and mode of analysis. A typical run time can be anywhere between 2 and 5 hours for analysis, depending on the resolution of the image required, covering ~200 frames, each 1.5 × 1.5 mm, with a typical resolution of 800 × 800 pixels. Sampling statistics are important and therefore the grid spacing used in, for example, point counting should be larger than the largest grain or particle size in the sample.

Mode of Analysis

The method of analysis is dependent on the information required and the methodology supported by the vendor software (Zhou and Gu 2016). All methods generally use a combination of BSE and EDX spectrum data measurements. Overall, a large number of points can be analyzed using a BSE image than by X-rays (e.g., 819,200 pixels vs. 40,000–60,000 X-ray points in 100s). However, the accumulation of X-ray data can be reduced by increasing the number of detectors used on the instrument and the development of methods in combining low-count X-ray data from various analyses (Gottlieb et al. 2015). Spatial resolution is also higher for BSE imaging than X-ray analysis with a resolution of between 0.1 and 0.2 μm compared to between 2 and 5 μm for X-ray analysis. However, difference in particles or grains cannot be distinguished by BSE where BSE intensities of the minerals of interest are similar (e.g., distinguishing different micas or clay minerals). The main measurement methods used in quantitative mineralogy systems are illustrated in Figure 8.

The technique used in a TIMA is illustrated in Figure 9. The image is divided into different segments. Each segment is assigned to a mineral or left unclassified. Adjacent segments located within a single particle are classified as the same mineral and joined to define a grain. For each grain, the total number of pixels within each segment and the mineral name is registered. The number of pixels for a specific mineral is derived as a sum of pixels of each grain that is assigned to that mineral. The relative volume and mass are then derived using the number of pixels.

Two approaches to analyses designed for speeding up the analysis are the bright phase search and the line scan mode. The bright phase search mode uses the backscatter brightness distribution obtained from the backscatter detector on the SEM to filter out particles that contain minerals of interest with high BSE contrast. This method eliminates analyzing grains that are of no interest and thereby reducing the analysis time. This is useful for searching sparse mineral phases such as gold and platinum group metals (PGMs) as described later.

For line-scanning mapping, the electron beam is scanned along in a series of lines across the polished mounts. The distance between adjacent horizontal lines and the distance between the measurement points along each horizontal line are defined. The lines are divided into linear sections divided by measurement points below the threshold to find sections through individual particles. The combination of the BSE level and the spectroscopic data can be used to determine transitions between distinct phases. This method can be used to provide modal analysis, but is useful for mineral grain size analysis also described later.

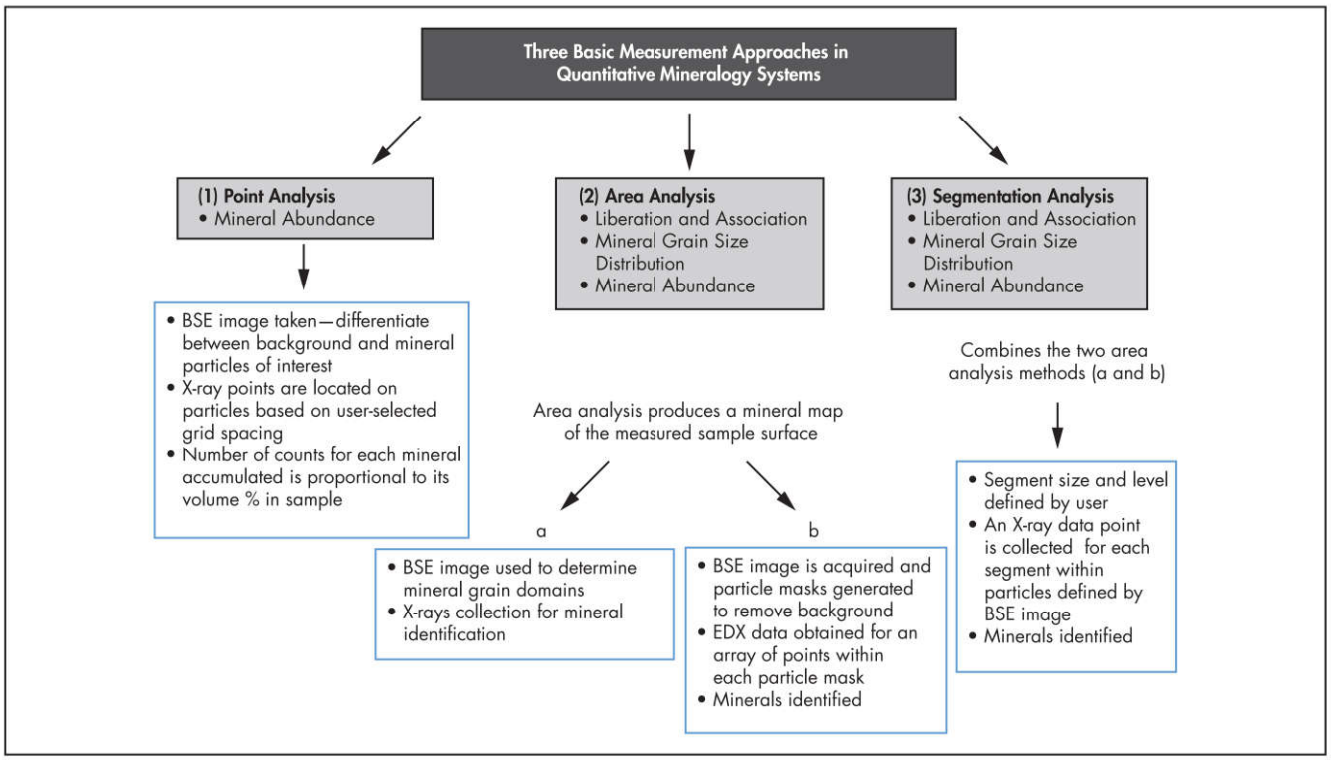

Source: Zhou and Gu 2016

Figure 8 Measurement approaches for quantifying mineral phases

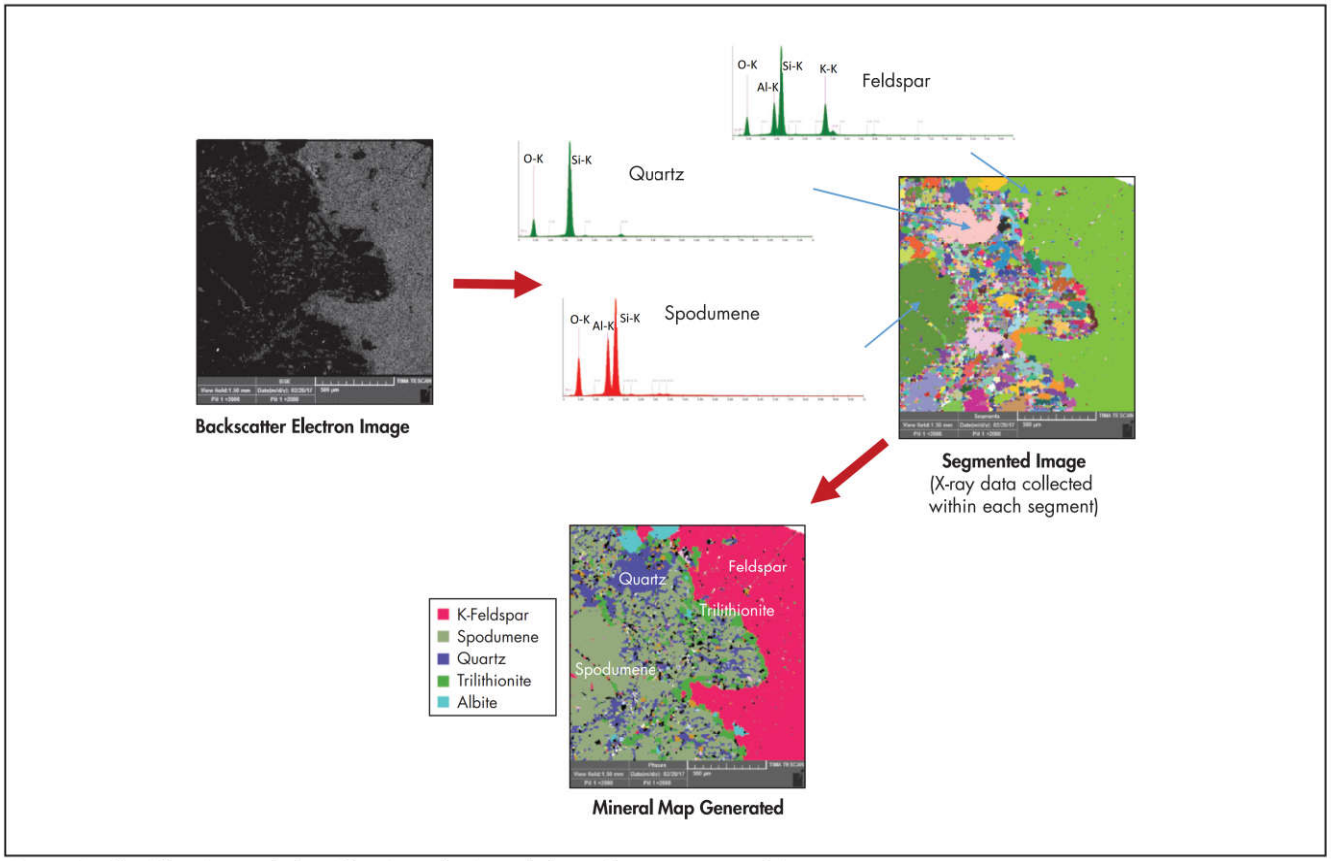

Figure 9 Identification and classification of mineral phase from segmented image

Classification of Mineral Phases

An important precursor to the measurement of ore characteristics in automated mineralogy analysis is the creation of the mineral library or mineral classification scheme, which represent the minerals expected in the ore or metallurgical sample that is being evaluated (Johnston 2016). Mineral classification by X-ray analysis is based on matching the entire spectrum of energy peaks collected on an unknown mineral to a library of X-ray spectra for known reference minerals collected under the same instrument parameters. The recorded backscatter intensity (gray level) can also be used to help distinguish the unknown mineral. Each mineral record in the library consists of a mineral name, chemical formula, density, X-ray spectra, and backscatter data. Ideally, the data collected for the listed minerals are from standards where the chemical composition has been determined by other analytical techniques (e.g., electron probe microanalyzer [EPMA], laser ablation–inductively coupled plasma mass spectroscopy [LA-ICPMS] described later). For minerals with variable compositions, specification of the elemental composition is more difficult, and some additional measurements may be required to determine an average value of the element in the mineral in the system.

Minerals that have large composition variations can be classified into two or more categories based on their composition ranges. Examples of where this is important in metallurgists' applications include defining sphalerite compositions with variable zinc and iron levels, siderite containing variable zinc levels, freibergite containing variable silver levels, and different types of pyrite grains containing arsenic and associated gold. In cases where fine minerals are intergrown and cannot be distinguished at the resolution of the SEM system, a phase mixture can be defined as a separate phase identity in the mineral library. The correct identification of silicate gangue minerals, such as clay minerals, talc, and pyrophyllite, is always important in leaching systems and froth flotation.

A condensed version of the minerals in the list can be generated by most automated systems. This is particularly useful in flotation applications where minerals can be grouped into nonsulfide gangue minerals, sulfide gangue, and minerals of interest categories. Such applications include bulk sulfide concentrate for gold and separation of copper minerals from pyrite and pyrrhotite and gangue minerals (Johnston 2016).

Type of Information Obtained by Automated SEM Systems

Following is a summary of the type of information that can be obtained from automated SEM systems, which is discussed in detail in the following sections:

- **Modal mineralogy.** The percentage of each mineral in the sample.
- **Elemental deportment.** The distribution of each element across all minerals containing that element.
- **Mineral liberation.** The distribution of the mineral of interest across particle composition classes, based on the bulk composition or surface composition of particles.
- **Mineral locking.** A measure of particle composition distribution based on quantifying the proportion of the mineral of interest.
- **Mineral association.** A measure of the degree to which pairs of minerals are adjacent to one another in the sample.
- **Mineral grain size.** Distribution of sizes of the grain cross-sections.
- **Phase specific surface area.** The surface area per unit volume of a mineral providing a single value, representing the mean mineral grain size distribution.
- **Particle shape.** Particle shape on a mineral-by-mineral basis that can be determined using a variety of conventional shape descriptors.

Importantly, in these analyses, the mineralogical identification and quantification is derived from compositional rather than structural analysis. Comparing quantitative XRPD with automated SEM analysis can therefore be valuable in identifying amorphous phases and correcting bias in either method.

Modal Mineralogy

A modal analysis is a listing of the minerals present and their mineral abundance expressed as weight percent. The volumetric fractions of each mineral are determined by converting the number of pixels of each mineral in a polish sectioned mount into the relative area as a percent. The sum of all relative volumes is calculated for all phases where the relative volume is equal to the relative area for a given phase (i.e., measurement from one-dimensional or 2-D mineral abundance data is equivalent to the true, 3-D value based on the Delesse principle). The relative mass of a phase as a percent is derived using the density value defined for each mineral in the mineral classification scheme. The smallest particle that can be measured is typically about 5 μm in size as the interaction volume of the electron beam is close to this size of the particle being analyzed.

The results can be presented in the form of analysis of different size fractions and whole sample as illustrated in Figure 10 for a crushed micaceous Li pegmatite. A typical table of modal analysis with errors is also shown. The relative error expressed as a percentage is calculated at the 95% confidence level (i.e., 2 standard deviations above and below the measured value; Napier-Munn 2014). Lepidolite represents a solid solution series between polylithionite and trilithionite and is defined as a composite in the mineral classification scheme.

The quality of the modal data depends on the reliability of the mineral recognition and the number of measurements made (Wightman et al. 2016). To increase the confidence of the user in the measurements produced, it is common to convert the mineral assays from an automated system to elemental assays, which are then compared with the independent elemental assays from a chemical laboratory.

Mineral Liberation Analysis and Characteristics

An understanding of the liberation characteristics or particle composition distribution of an ore is important in comminution circuit design and for optimizing beneficiation processes such as flotation, density, and magnetic and electrostatic separations in operating plants. This type of analysis can provide the metallurgist with details on what proportion of the valuable minerals are liberated, the amount of unliberated (composite) particles that require further grinding, and the proportion of the liberated gangue minerals that can be directed to the tails. Equally important is the understanding of how unliberated particles vary in composition and texture (Evans and Morrison 2016). The form of information required is dependent to some degree on which separation process is used to treat the ore and what physical property of the particles is required to be exploited in the process (e.g., surface area

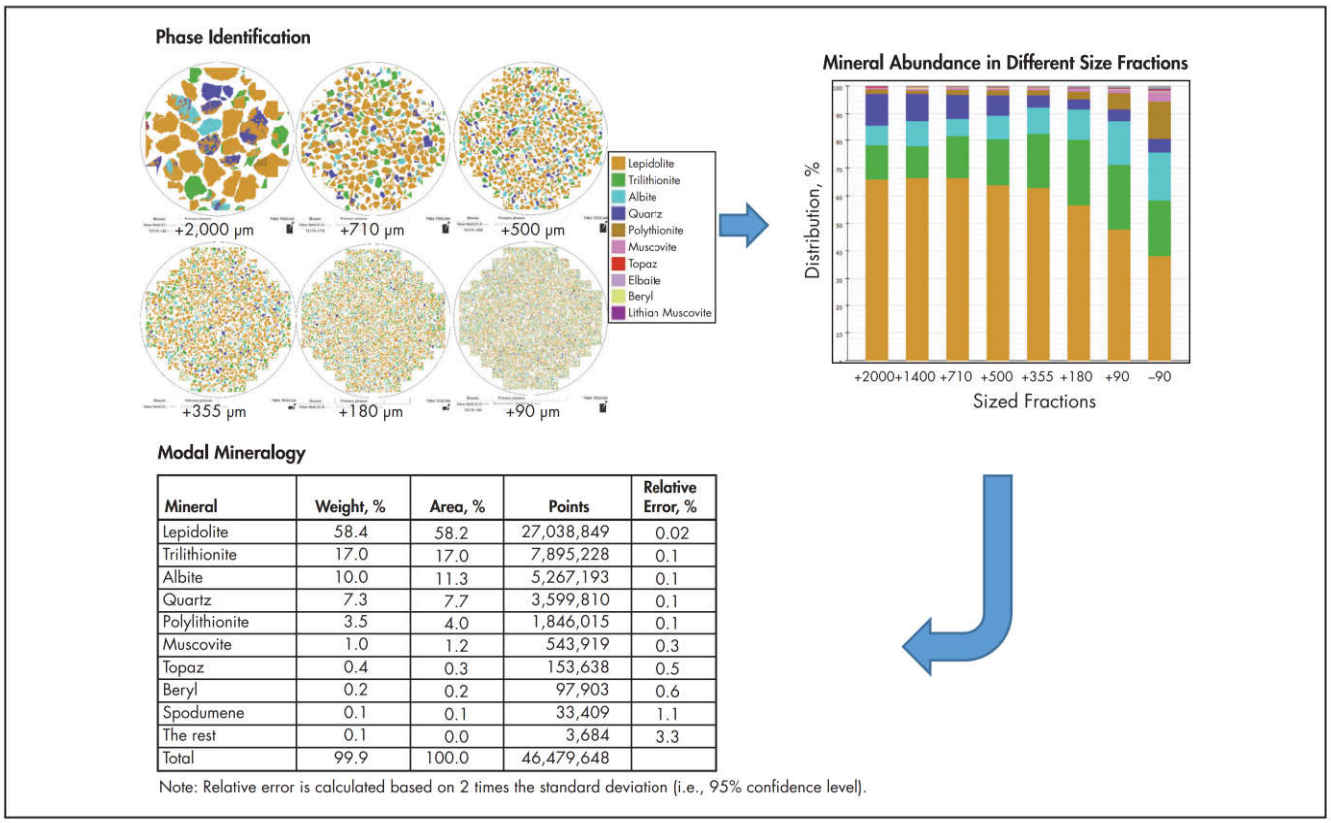

Modal Mineralogy

Mineral	Weight, %	Area, %	Points	Relative Error, %
Lepidolite	58.4	58.2	27,038,849	0.02
Trilithionite	17.0	17.0	7,895,228	0.1
Albite	10.0	11.3	5,267,193	0.1
Quartz	7.3	7.7	3,599,810	0.1
Polylithionite	3.5	4.0	1,846,015	0.1
Muscovite	1.0	1.2	543,919	0.3
Topaz	0.4	0.3	153,638	0.5
Beryl	0.2	0.2	97,903	0.6
Spodumene	0.1	0.1	33,409	1.1
The rest	0.1	0.0	3,684	3.3
Total	99.9	100.0	46,479,648	

Note: Relative error is calculated based on 2 times the standard deviation (i.e., 95% confidence level).

Figure 10 Modal analysis in sized fractions and whole sample for a crushed micaceous Li pegmatite

exposed for leaching and flotation, volume for gravity or magnetic separation techniques). In automated SEM techniques, the liberation of a particle with respect to a given mineral of interest can be computed and expressed in one of the two following forms:

1. **Surface area.** Liberation of a particle is the length fraction on the outer perimeter of the particle covered by a mineral(s) of interest with respect to the whole outer perimeter of the particle expressed as a percentage.
2. **Volume.** Liberation of a particle is the area fraction of a mineral(s) of interest with respect to the total area of the particle normally expressed as a percentage.

Mineral *locking* expresses which phases a mineral of interest is locked within and how much free surface is exposed. The level of locking is a function of the surface area of a particular mineral. Overall, while the liberation characteristic function provides information on the composition of the mineral of interest, the mineral locking function provides information on the texture of each particle.

Mineral association yields information about spatial relation between phases inside particles. This analysis reports the percentage of the mineral of interest that is fully liberated, in binary and in ternary particles. However, reporting the mineral associations as a modal analysis for each liberation class is advised for concentrator plants (Lastra and Paktunc 2016).

To obtain accurate liberation data, samples are sized and polished mounts are made of the different size fractions to be measured separately. This is to reduce the stereological bias that is inevitable when attempting to measure 3-D objects with their 2-D sections (Spencer and Sutherland 2000). The magnitude of the stereological bias is small for particles with complex textures, reaches a maximum for a given ore for binary particles with simple texture, and then reduces to zero for particles that are fully liberated (Gottlieb et al. 2000; Spencer and Sutherland 2000; Evans and Morrison 2016). Fortunately for most systems with a natural range of particle composition distributions, the measured liberation characteristics have been observed to be similar to true liberation values, and only systems with narrow composition ranges require major adjustments (Petruk 2000).

For liberation analysis, it is important to remove agglomerated particles. Agglomerated particles affect the results of mineral liberation assessment, because they are considered as one particle. Samples of dry flotation concentrates commonly have agglomerated particles. Samples can be subjected to a strong attrition treatment process (e.g., ultrasonic bath) to remove the agglomerated material prior to mounting. Alternatively, many automated software systems have particle separation routines that set boundaries between touching particles within agglomerates.

For analysis, the particles are divided into composition or surface exposure bins based on their liberation. Figure 11 illustrates a liberation analysis for sphalerite in a massive sulfide sample expressed as cumulative liberation yield of sphalerite by particle surface area, theoretical grade–recovery curve, and as a graphic representation in terms of degree of liberation and size. In this example, the data is separated into 10 bins at 10% intervals, representing particle surface area liberation classes (≥0 and <10%, ≥10 and <20%,

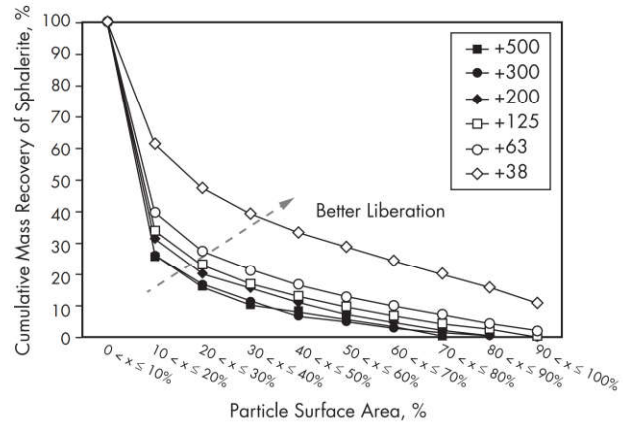

A. Cumulative liberation yield of sphalerite by particle surface area for different size fraction

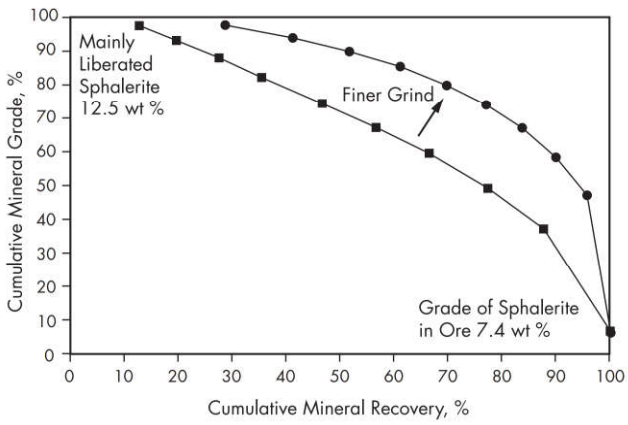

B. Theoretical grade–recovery curve; finer particles offer higher liberation of free grains of sphalerite (arrow)

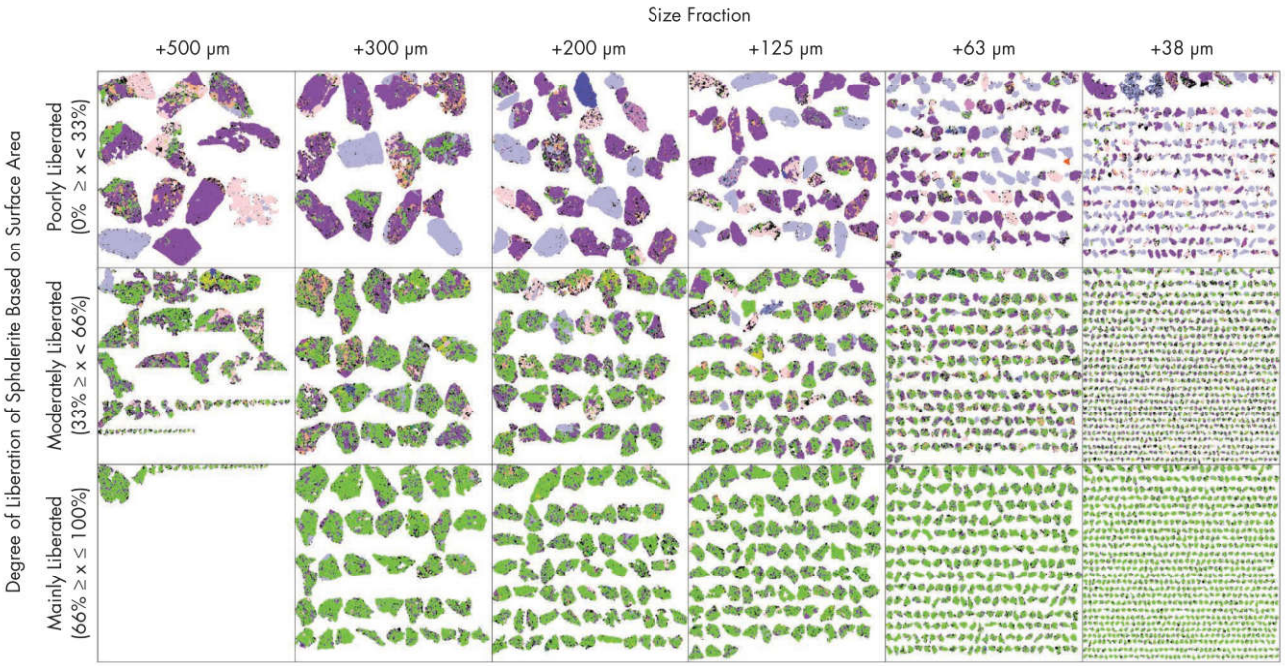

C. Degree of liberation of sphalerite represented graphically in different size fractions

Figure 11 Liberation analysis by surface area of sphalerite in a Zn-Pb massive sulfide sample

etc.) for different sized samples, and shows finer grain size promotes exposure of more separate sphalerite grains for beneficiation.

Grade–recovery curves are a common method for representing the performance of industrial flotation operations and batch flotation tests, for example, the liberation of sphalerite in a Zn-Pb massive sulfide sample (Figure 11B). The theoretical grade–recovery curve for an ore is defined as the maximum expected recovery that can be achieved by physical separation of a mineral at a given grade (McIvor and Finch 1991). This is determined by the surface area liberation of the mineral of interest and is directly related to the grind size. A combination of automated mineralogy SEM and flotation test work can be used to define the efficiency of a process and allow for the diagnoses of where potential improvements may be made. The position of a theoretical grade–recovery curve is calculated based on liberation values and the mineral assay data that is sorted by the software in descending order of particle quality. In most automated SEM software, the data can also be screened or filtered to categorize particles or mineral phases and then be visually displayed (Figure 11C).

The disadvantage of producing five or six sized subsamples instead of one sample for liberation studies is that the cost of the study can be expensive. In some circumstances, it is possible to use uncorrected liberation data from unsized samples for comparative studies where samples have been taken from a single process operation (Lastra and Petruk 2014).

Theoretical grade–recovery curves provided by automated mineralogy techniques are generated from 2-D liberation measurements and overestimate the true liberation by a certain amount and therefore only provide a guide. Test work is always required to validate the results.

Mineral Grain Size and Shape Analyses

Automated imaging systems can be used to assist in the measurement of grain size as part of the property describing ore texture. Mineral grain size distribution data are a useful predictor of liberation when developing or modifying existing comminution circuits (McIvor and Finch 1991; Evans and Wightman 2009; Johnston 2016).

Grain sizes should ideally be estimated by measurements on polished mounts of rock samples or blocks of ore that are significantly coarser than the mineral grains of interest (Sutherland 2007). Direct estimate of the grain size can be made by measuring the equivalent circle diameter and maximum diameter of a grain particle. However, this approach is stereologically biased because of the sectioning of grains in the polished mount where the 2-D image of grains represents less than or equal to the true size of the grain. The phase specific surface area (PSSA) measurement function can be used and is not stereologically biased. To collect data for grain size estimation using line scan measurements (line scan mode) is preferred over area image mapping. The parameter provides a single value representing a mean grain size of each mineral in a mount but does not use actual grain measured distribution. Overall, estimation of grain size distributions should be used with caution and in conjunction with the PSSA for each mineral. The results should be collated and cross checked with actual experimental data for validation.

In some software systems, such as MLA, the grain shape can be measured in terms of aspect ratio, shape factor, and angularity (Tsikouras et al. 2011). Particle shape analyses, along with the measurement of porosity, are particularly useful in sedimentary rock studies such as those used in the oil and gas industry.

Statistical and Error Analysis

When comparisons are being made between different size fractions in grinding and flotation circuits, it is useful to quantify the errors in the measurements to determine whether any differences are significant. As the particle size increases, the number of measured particles decreases, which is caused by limitations in the number of particles that fit into one polished block. The reduction in the number of particles measured increases the errors associated with the measurement, and therefore multiple polished blocks may be required to be measured. As many processes are now investigating coarse rejection of gangue as a method to reduce operating costs, the analysis of coarse particles is becoming more prevalent. Based on statistical analysis by various workers, at least 2,000 particles are required to be measured in polished mounts (Evans and Napier-Munn 2013; Mariano and Evans 2015). Alternatively, combining and reducing the particle composition class in the distribution increases the number of particles in each composition class, is also effective, and allows for the reduction in costly analytical time.

Analysis of Low-Grade and Precious Metal Ores

One of the main advantages and applications of automated digital mineralogy techniques is in the measurement of low-grade components in samples, particularly in analyzing precious metals (PGMs and gold) or for investigating indicator minerals (e.g., zircons or rutile) in exploration studies. The benefits of the use of automated mineral mineralogy techniques and some of the challenges in gold deportment studies have been discussed in the literature (Chryssoulis and Cabri 1990; Goodall 2008; Chryssoulis and McMullen 2016).

In gold metallurgy studies, the feed and tailings gold grades are generally very low (<10 ppm), and the low frequency of occurrence of grains containing target minerals means that they are difficult to locate in statistically representative numbers.

Normally, both free gold and sulfide mineral grains associated with gold have a higher density compared with the gangue minerals. This allows for them to be concentrated using techniques such as a shaking Wilfley table or gravity gold recovery test (Laplante et al. 1995) for coarse-particle analysis. For finer particles, a combination of heavy liquid separation (bromoform, 2.889 g/mL; methylene iodide, 3.325 g/mL; water-based Li polytungstate solids, 1–2.95 g/mL) and super-panning (Zhou and Cabri 2004), as well as hydroseparation techniques (Lastra et al. 2005; Cabri et al. 2005, 2008), depending on the type of sample under investigation, can be used to concentrate and improve the efficiency and representation of the analysis. However, care must be taken that gold grains associated with gangue minerals are not discounted from the final gold balance. Coarse free gold minerals are usually best identified by reflected light microscopy as stereomicroscope provides 3-D vision about the flakiness of gold grain (Chryssoulis and McMullen 2016).

In the determination of gold and PGM deportment studies, bright phase search mode is used where each of the fields on the polished mount are fast scanned for precious metals (gold or PGMs) based on the backscatter brightness distribution obtained from the backscatter detector on the SEM. The BSE brightness threshold in the software is set at a level that filters out particles that contains minerals of interest and eliminates analyzing grains that are of no interest. This helps reduce the analysis time. The practical limit of detection for gold grains is 1–2 μm by this method but is dependent on the step size used in the scanning grid. Once a bright phase is found, the whole host particle can be mapped to yield information about the mineral association. Some bright-field scanning modes have been developed to allow more detailed evaluation of grains (e.g., liberation, second grain mapping) such as found in the MLA software (Fandrich et al. 2007). An example of output using the bright phase search in the TIMA is shown in Figure 12, where the grains containing detected gold, sylvanite, and their mineral associations can be listed and documented.

Minerals such as galena and bismuth, however, which also contain high BSE brightness values close to that for gold can cause an issue, which means they also are detected and analyzed along with gold. This is prevalent when analyzing materials such as auriferous massive sulfide Zn-Pb deposits that can have finely disseminated galena grains within pyrite grains. Hence, BSE brightness threshold setting needs to be set to filter out other bright-field minerals.

Although automated mineralogical image analysis can be used to define the mode of gold grain occurrence, associations, and gangue mineralogy, target sulfide minerals must be identified and selected for analysis of submicroscopic gold concentrations by microbeam and surface analysis techniques

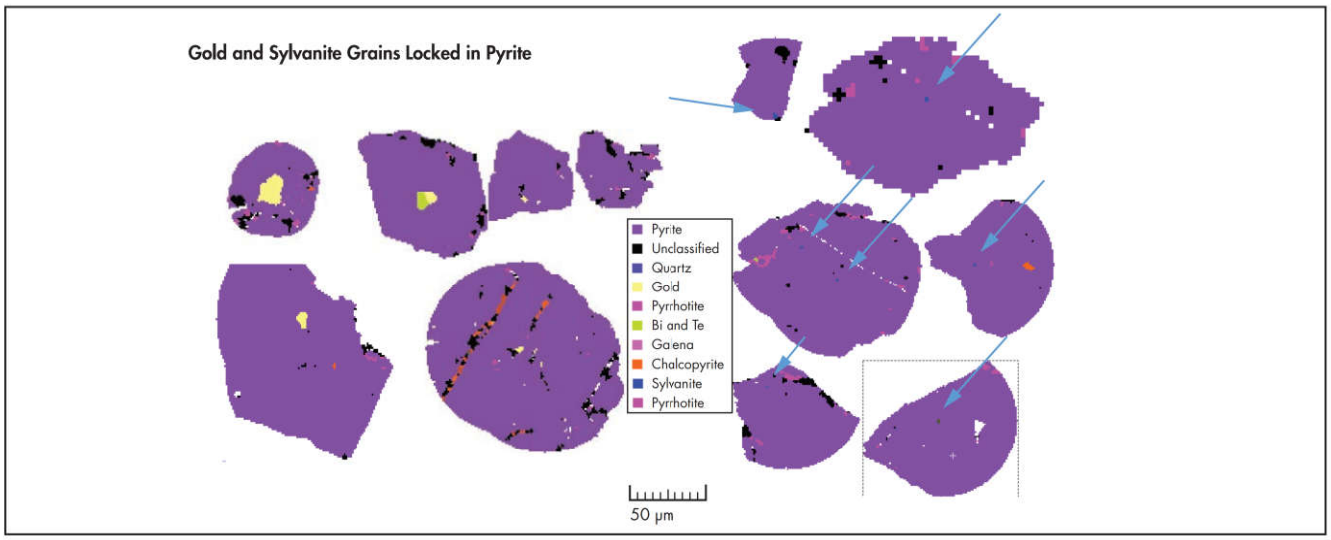

Figure 12 Pyrite particles containing gold (light) and sylvanite $(Au,Ag)_2Te_4$ (arrows) grain inclusions

described in the "Semiautomated Microprobe Techniques" section. The combination of the abundance and textural types of gold carriers determined is then used to calculate the cumulative gold concentration in the sample. Combining automated mineralogical techniques with diagnostic chemical assaying has also been effective in applications, such as in analyzing a flotation tailings stream of a Cu–Au operation in North Queensland, Australia, where gold loss was determined to be caused by the presence of coarse free gold (Goodall 2008).

Bright phase search can also be effective for uranium ores for locating uranium minerals, although there, abundance is much higher compared to gold grades.

Main Sources of Error and Limitations in Quantitative Analyses

Although automated quantitative mineralogy estimation provides a powerful tool for analysis, the accuracy and data interpretation depends on many operator, physical, chemical, geological, sampling, and statistical factors. Some sources of error and limitations are as follows:

- The analysis of data requires some knowledge of mineralogy, metallurgical, and geological processes when training the system and interpreting the results, not simply automatic readout of data.
- An understanding of basic physics concepts in accounting for the spatial resolution limitations of electron-induced X-ray emissions (energy, density, and generation volume) is important, particularly as they vary with the composition of phases under examination.
- The quality of the data in the mineral classification scheme (library) used in automated SEM systems for identifying minerals is validated and is clearly documented where the data and information originated. Mineral abundance, assay reconciliation, and mass balancing are reliant on the library data.
- Correct sample selection, subsampling, and processing of the samples ensure that the right sample is analyzed. The sample preparation, knowledge, and skill in creating representative polished sections is also important.
- Appropriate measurement mode, pixel spacing, and measurement time must be selected. The conditions used have to take into account the available time as well as application.
- Estimates for 3-D properties from 2-D measurements (stereology) are limited. The results should always be checked with experimental data to ensure continuity.
- Lack of information in estimating the proportions of low-atomic-number elements from EDX spectra (absorption of low-energy photons by the detector window) can result in error. The data for elements below and including carbon are not or are only partially represented in EDX spectra, which can reduce its effectiveness in classifying some mineral phases (e.g., Li in spodumene, carbon in carbonate minerals).
- The overlapping of some X-ray lines can reduce detection for some elements, such as rare earth elements in monazite or between Pb and S in galena, and ultimately the identification of the mineral phase.
- Minerals should not be identified based on their chemical composition alone (e.g., polymorphs aragonite and calcite, sphalerite and wurtzite).
- Interaction volume can result in a mixed spectrum of minerals for complex samples.
- The practical limitation of grain identification is ~0.5 µm.

Applications

Applications of the use of automated SEM are well documented in the literature for just about every metal commodity. A recent book published on process mineralogy provides many detailed applications where automated mineralogy has been used in industry (Becker et al. 2016). Other applications have included the characterization of Ni-rich and Ni-poor goethite in laterite ores (Andersen et al. 2009) and rare earth element deportment studies (Smythe et al. 2013). A selection of results illustrating the usefulness of automated digital mineralogy is shown in the following subsections.

Liberation Analysis of Sulfide Minerals

The application of automated mineral techniques in optimizing the liberation of sulfide components in concentrators from

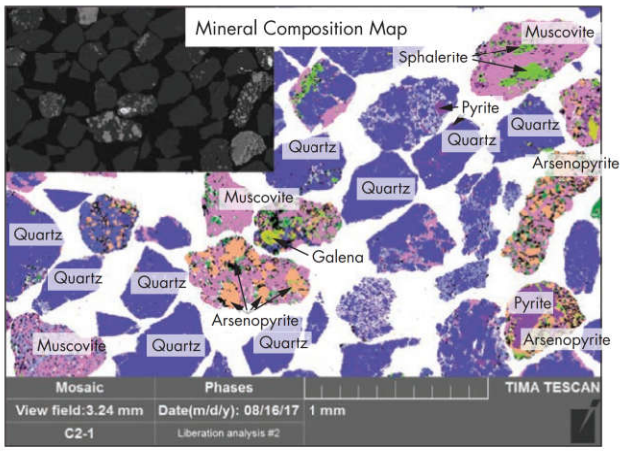

A. Mineral map with embedded backscatter image

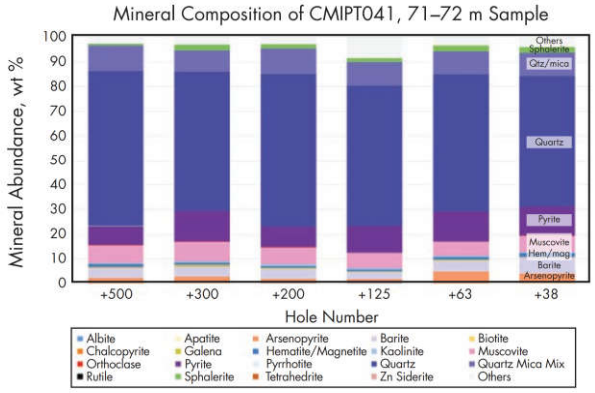

B. Modal mineralogy of different sized fractions

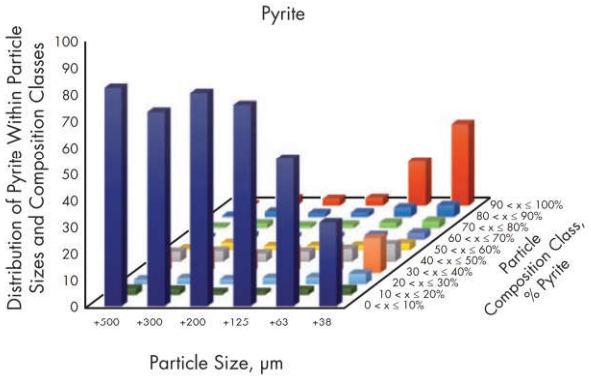

C. Measured particle composition distribution for pyrite

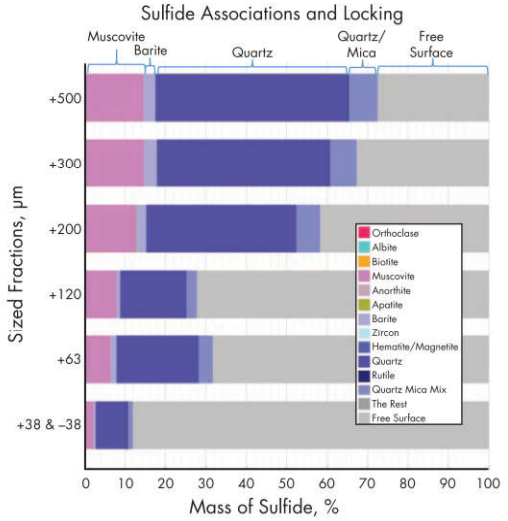

D. Proportions of sulfide minerals free and locked in gangue minerals

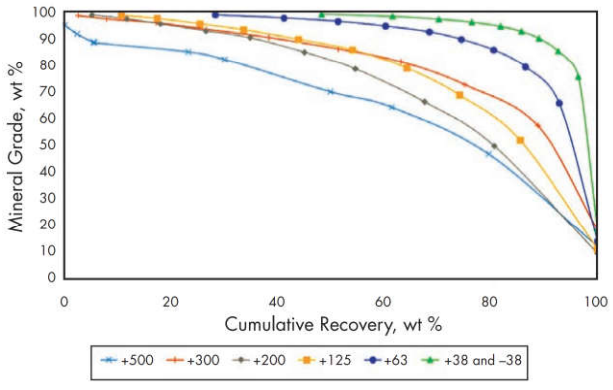

E. Theoretical grade–recovery curve for sulfide minerals

Figure 13 Mineral liberation analyses of a feldspar porphyry rhyolite-rhyodacite sample

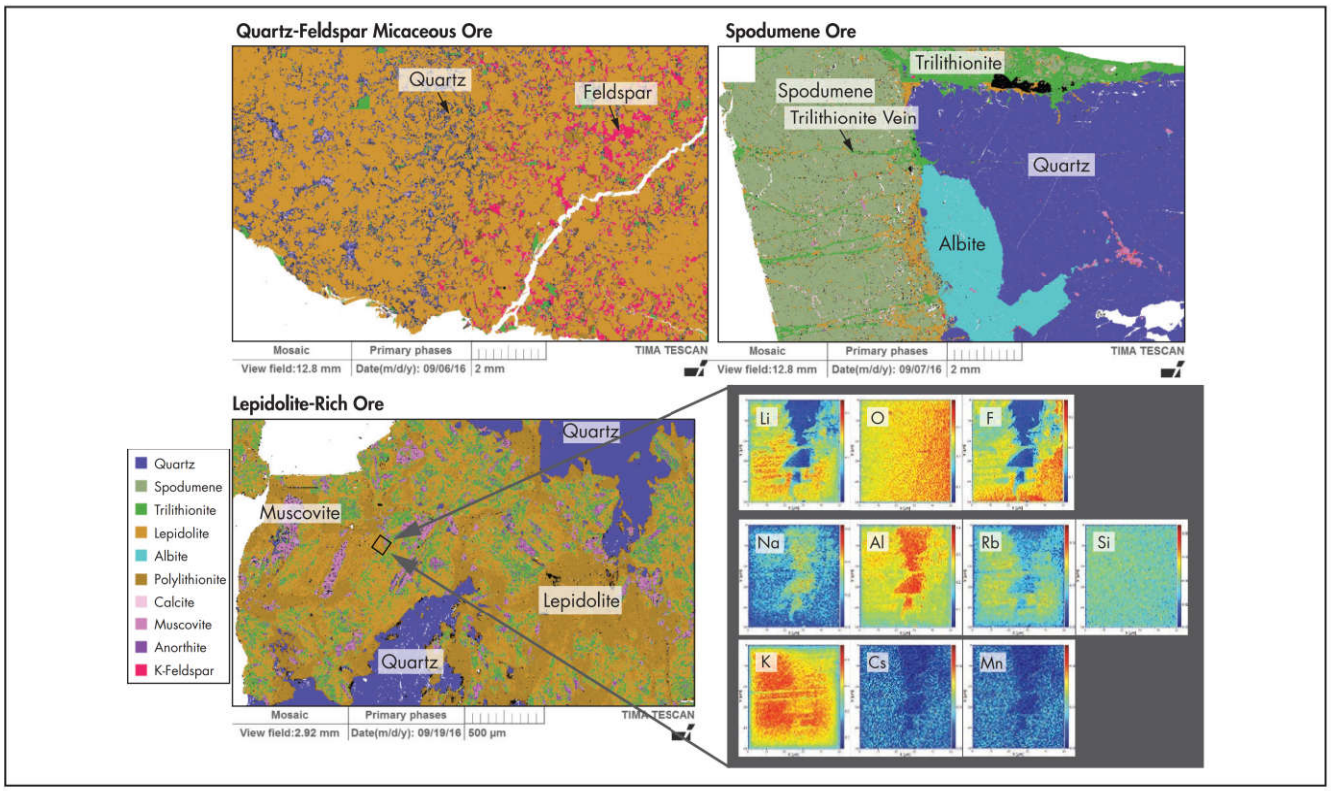

Figure 14 Mineral composition maps for three different textured lithium-bearing pegmatites with time-of-flight secondary ion mass spectrometry analysis

Zn-Pb sulfide ores (e.g., McKay et al. 2007; McKay 2016; Fosu et al. 2015; Johnston 2016) and copper ores (MacDonald et al. 2011) are documented in the literature. Figure 13 illustrates partial results for an assessment of a feldspar porphyry rhyolite-rhyodacite deposit showing the mineral composition map, the modal mineralogy, and the liberation and concentration of sulfide minerals for gold recovery. LA-ICPMS analysis performed on the sulfide grains indicated solid solution gold in pyrite (averaging 4.8 ppm, 0–15 ppm) and arsenopyrite (averaging 86 ppm, 0–550 ppm) grains. A backscatter micrograph together with the mineral map image and modal mineralogy for different sized fractions illustrates most of the sample is made up of silica minerals (Figures 13A and 13B). The particle composition distribution for pyrite results was obtained using the mineral liberation function in the TIMA software. The amount of the major sulfide minerals in each particle composition class, ranging from 0% to 100% in 10% intervals, was calculated for each of the particle size fractions. The measured particle composition distribution for pyrite, the assessment of the amount of sulfide minerals locked in gangue minerals, together with the theoretical grade–recovery curve for sulfide minerals are presented in Figures 13C–13E. Overall liberation analysis generated from the data shows most sulfide minerals are in composite grains with quartz and muscovite, mainly in the coarse-size fractions, and require fine grinding to liberate particles.

This information along with other information on mineral deportment, their size distributions, compositions, and associations with other minerals are being used to assess the economic viability to treat this ore.

Lithium Ores

The demand for lithium has increased significantly in recent years as a result of an increase in demand for lithium-based rechargeable batteries for portable electronic devices and electric passenger cars. Hence, a comprehensive understanding of the deportment of lithium and associated minerals in potential ore bodies is essential to allow the industry to predict the response of ore reserves to metallurgical treatment options. Figure 14 illustrates the complexity of mineral intergrowths in some potential lithium-rich ores using the high-resolution mapping scan mode of TIMA and the integration of techniques such as time-of-flight secondary ion mass spectrometry (ToF-SIMS) to allow for the measurement and correlation of lithium (not measured with standard EDX spectrometry) and other elements associated within different minerals. The mineral composition maps illustrate lepidolite, a lithium-bearing mica, intergrown with quartz and feldspar in a quartz-feldspar-micaceous sample; a spodumene grain with fine veins of lithium-bearing micas (lepidolite, trilithionite) attached to quartz and albite in a spodumene ore; and a lepidolite-rich sample, showing alteration to muscovite. The ToF-SIMS elemental scans illustrate lithium is associated with F, enriched K, Rb, Cs, and Mn in lepidolite; and muscovite is deficient in Li and associated with Na and high Al content. The characterization of different lithium minerals in pegmatite ores and its implication to processing have been published elsewhere (Aylmore et al. 2018a, 2018b).

Precious Metals Deportment Studies

Automated SEM techniques can be used to determine how much gold and silver is free or liberated and what percentage

is attached to each of the major minerals such as galena, chalcopyrite, sphalerite, pyrite, and nonsulfides. There are many examples that can be found in the literature (e.g., Goodall et al. 2005; Goodall and Butcher 2012). Figure 15 illustrates results from using bright-field scans and detailed mineral map scans in the high-resolution mapping mode of TIMA to assess precious metal content in six mounts on a massive sulfide flotation feed (Au 1.8 g/t, Ag 140 g/t, 13.6% Fe, 19.4% S). Coarse gold associations and one of the silver-bearing minerals observed, together with their energy spectrum analysis and chemical composition analysis, are illustrated in the figure. The deportment of silver in different minerals and their associations with other minerals is also shown. The results indicated the potential for gravity recoverable gold, whereas silver is present in several different minerals in the ore.

Carbon Analysis

A combination of reflected light microscopy and automated SEM analysis have been used in the determination of mineral characteristics of carbon materials such as coal (O'Brien et al. 2011; Van Alphen 2007; Gottlieb et al. 1991). Coating or mounting samples in carnauba wax is often done when preparing coal samples, as the BSE image provides better discrimination between the mounting medium and the coal particles. In some cases, the chemical signature of the resin can be sufficiently different to carbonaceous material to allow for particles to be differentiated. Figure 16 illustrates mineral compositional maps of in polished cross-sectional mounts of rock and fragmented sample showing graphite particles (dark gray) distinguishable from the resin (light gray).

SEMIAUTOMATED MICROPROBE TECHNIQUES

Automated mineralogical systems require a mineral library with elemental compositions of minerals expected in the ore or residue of interest. Although literature references will provide a basis for these calculations, variations in composition and low-level solid solution values within some mineral species require the use of other analytical electron beam techniques. For accurate mass balance derivations and deportment, assessments require quantitative compositional analyses, which can be obtained by techniques briefly described in the following subsections. Detailed compositional data yielded from microprobe analysis and mass spectroscopy techniques can be entered back into the automated mineralogy software, and mineralogical measurements can be reclassified to update overall modal and deportment data. The suitability of a technique for analysis is dependent on the detection limits and spacial resolution of microbeam techniques used.

Electron Microprobe with Wavelength-Dispersive Analyses

EPMA, using such equipment as a Cameca SX-100 electron microprobe, can be used to acquire precise, quantitative analyses of major elements down to trace with high spatial resolution spot sizes in the order of 100–200 nm in modem FEG-based instruments. Individual grains and textures as small as 2–5 μm can be targeted (Pownceby and MacRae 2016). The high electron beam currents and beam stability of EPMA, coupled with high-resolution WDX spectrometry, allow for detection limits and accuracy to 100 ppm for trace element compositions within many mineral species.

EPMA has the same basic principle of operation as SEM, except EPMA is designed primarily as a quantitative tool. Modem EPMA instruments are usually outfitted with one or more EDX spectrometers as well as an array of several WDX spectrometers mounted to the column for the simultaneous measurement of multiple elements (Pownceby and MacRae 2016). Samples supplied as carbon-coated, polished sectioned mounts prepared for automated mineralogy can be analyzed and allows the same sample to be analyzed using the two techniques.

In comparison with EDX spectrometers, WDX spectrometers have the advantage of superior peak resolution, high peak-to-background ratios, and minimal problems of overlapping X-ray lines, which provides better detection for some elements such as rare earth elements in monazite, or between Pb and S in galena, and trace elements. High count rates (>100,000 counts/s) can be accommodated by WDX spectrometers without loss of peak resolution, which allows them to detect elements at an order of magnitude lower in concentration than can be detected by EDX spectrometers. However, X-ray data can only be obtained for one element at a time, with each element's spectrum acquired sequentially as the wavelength range is scanned, which means acquisition time, particularly in a complex mineral with many elements, can take longer for collection and analysis of data. Recent development of silicon drift detectors, which offer high throughput and improvements in resolution, have led to routine analyses at detection limits in EDX spectrometers approaching that of WDX-based analysis.

The measured X-ray intensities from the detectors are corrected for X-ray absorption, secondary fluorescence, and electron backscattering using one of the matrix correction methods (Pouchou and Pichoir 1985; Armstrong 1988; Goldstein et al. 2003). For quantitative microanalysis, a comparison of X-ray emission from the unknown specimen with that from one or more SRMs of known composition is made. SRMs are readily available for this type of analysis.

Laser Ablation–Inductively Coupled Plasma Mass Spectroscopy

For minerals that require a measurement with a lower detection limit than can be provided by EPMA, LA-ICPMS can be considered (e.g., Cabri et al. 2010; Bowell et al. 2005). Inductively coupled plasma mass spectroscopy (ICPMS) is one of the most important analytical techniques available for trace element analysis, mainly because of its high degree of accuracy and precision. The mineral samples can be thin or thick sections or polished mounts of different dimensions, such as those for automated SEM applications. LA-ICPMS can have sub-parts-per-million sensitivities for elements such as rare earths and one part per million for most elements of the periodic table. However, it has a very large microanalytical volume, which can limit the grain size evaluated and resolution.

LA-ICPMS systems consist of a laser ablation unit and a mass spectrometer. (Klemd and Bratz 2016). The most widely used laser ablation systems are either the solid-state Nd-doped, Y, Al, garnet (Nd:YAG) using a wavelength of 266 nm or 213 nm and the 193-nm excimer gas laser ablation system. The Nd:YAG systems are cheaper and designed to cover a large range of applications such as ablations of metals, ceramics, plastics, glass, coatings, minerals, and environmental matrices. However, the use of shorter wavelength sources improves the absorption of the laser radiation and the resulting

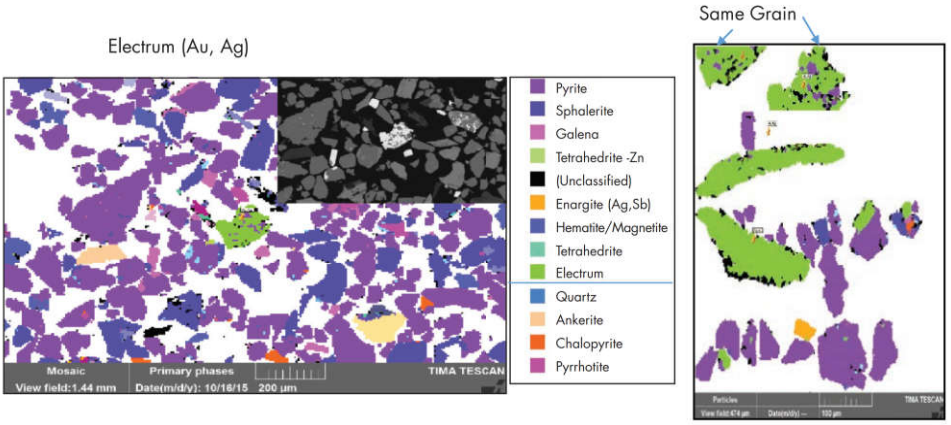

Element	Electrum, wt %	Average Composition, wt %	Range, wt % (8 grains)
Ag	>20	53.8	39.6–63.4
Au	<80	45.4	59.3–36.2
Fe			0–2.5

A. Free electrum grains with chemical analysis

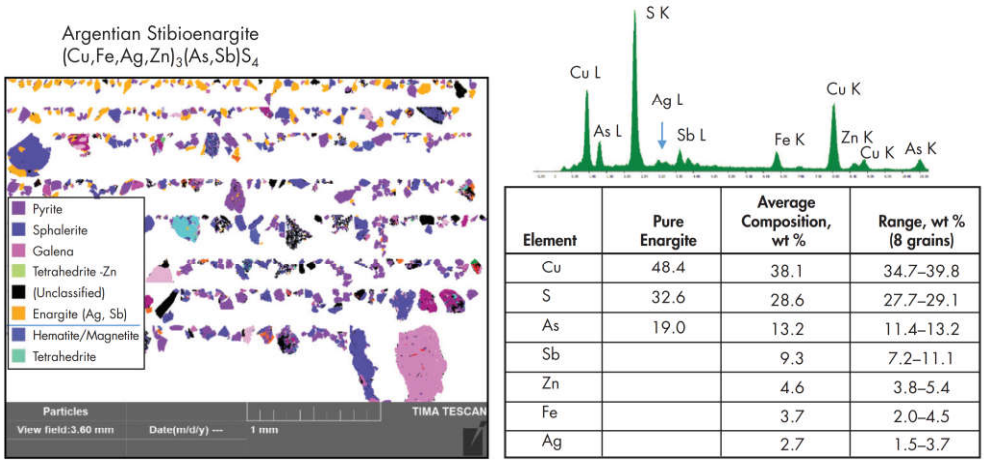

Element	Pure Enargite	Average Composition, wt %	Range, wt % (8 grains)
Cu	48.4	38.1	34.7–39.8
S	32.6	28.6	27.7–29.1
As	19.0	13.2	11.4–13.2
Sb		9.3	7.2–11.1
Zn		4.6	3.8–5.4
Fe		3.7	2.0–4.5
Ag		2.7	1.5–3.7

B. Enargite with energy-dispersive X-ray spectrum and chemical analysis

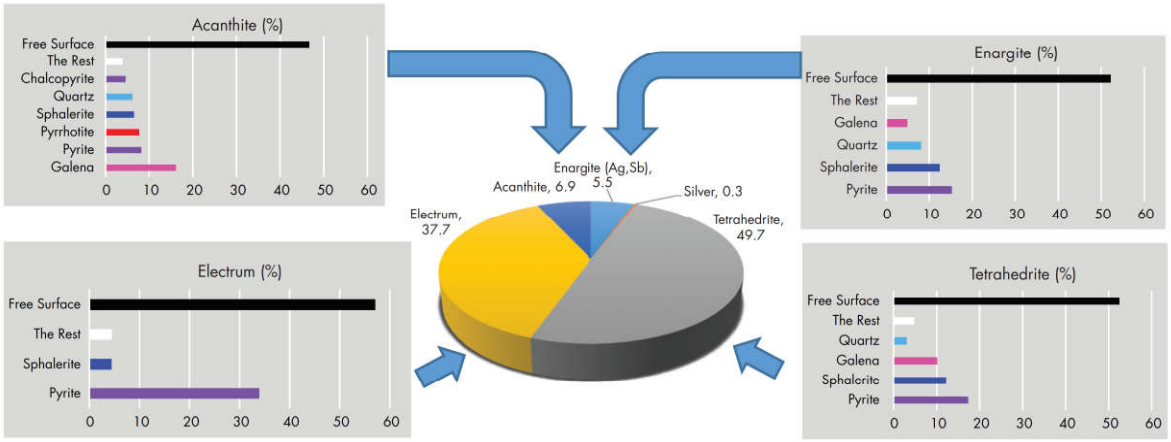

C. Deportment of silver and mineral associations

Figure 15 Gold and silver deportment, mineral analysis, and associations in a massive sulfide flotation concentrate

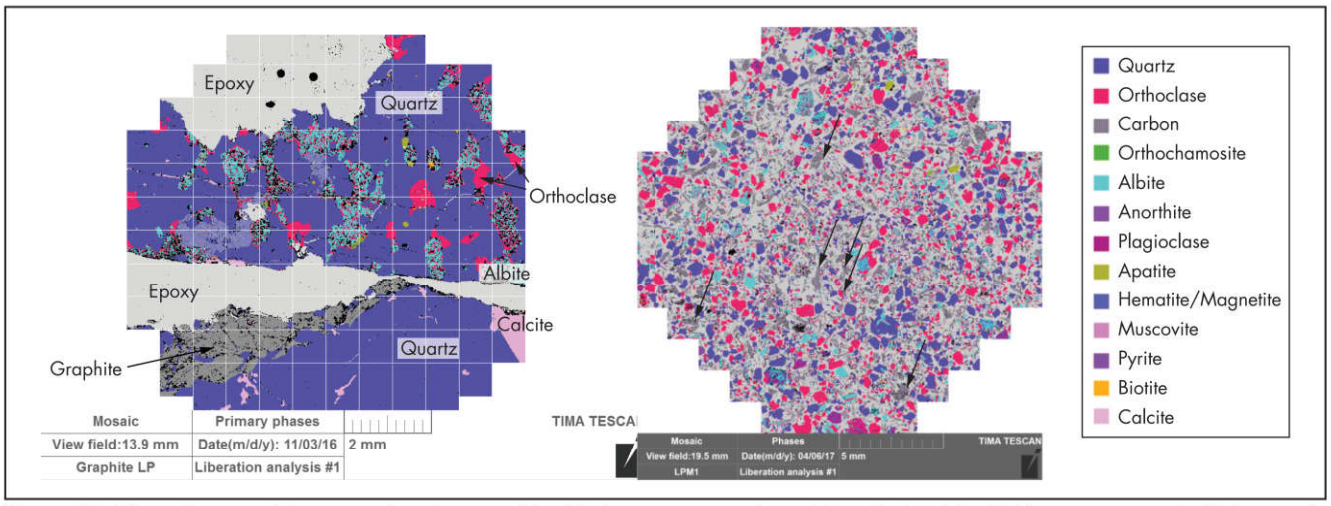

Figure 16 Mineral composition map showing graphite (dark gray; arrows) particles distinguishable from epoxy resin (light gray)

ablation characteristics, especially for colorless minerals and materials.

The laser beam is focused on the sample surface and vaporizes and partially ionizes the material at a spot on a particle. Both spot and detailed mapping analysis can be carried out on different mineral grains or particles. The diameter of the laser beam (1–400 μm), the repetition rate (1–100 Hz), the irradiance (measured in gigawatts per square centimeter), and the fluence (measured in joules per square centimeter) are variables that are adjusted for different applications. The signal intensity obtained for the respective elements is directly proportional to the amount of ablated material transported to the ICPMS. Quadrupole and single collector instruments are normally used for quantitative (moderate-high precision) element analyses. Multicollector magnetic sector field instruments are able to simultaneously determine isotope ratios at a very high precision (Harris 1998; Longerich 2008).

The main issue with LA-ICPMS analysis is the availability of suitable matrix-matched standards, which are essential for the calibration of the elemental analyses and in the destructive nature of the technique.

HIGH-RESOLUTION X-RAY COMPUTED TOMOGRAPHY

The application of high-resolution X-ray computed tomography (XCT) or micro-CT, a nondestructive 3-D imaging and analysis technique for the investigation of internal structures of large objects, has increasingly gained interest as a mineral characterization tool in geoscience and metallurgy applications (Cnudde and Boone 2013; Miller and Lin 2018). XCT consists of an X-ray source, a series of detectors that measure X-ray intensity attenuation along multiple beam paths, and a rotational geometry with respect to the object being imaged. Based on the magnitude of the X-ray attenuation coefficient, differentiation of mineral phases within the sample is possible. A specialized algorithm is then used to reconstruct the distribution of X-ray attenuation in the volume being imaged.

X-ray tomography has been used to quantify particle size, shape, and composition, based on the linear attenuation coefficient of particles as X-rays pass through a sample. Applications to the study of particle fractures resulting from blasting and comminution; liberation characterization to describe expected separation efficiency; grain surface area analysis to explain the flotation of locked particles; and floc size, shape, and water content for polymer-induced flocculation, have been described by Miller and Lin (2018). XCT provides a complementary technique to automated SEM systems in that larger sample volumes can be observed by XCT, and particle size and shape analysis are not affected by stereographic issues, whereas automated SEM systems can provide accurate mineral identification and high-definition images to calibrate mineral identification in XCT images. Recent developments in the use of dual-energy XCT, where two X-ray images at two different X-ray energies are collected simultaneously or sequentially, improves the range of mineral densities that can be measured to aid in differentiating between minerals (Lin et al. 2013; Wang et al. 2014). Recent advances in XCT instruments have included high-speed scanning and image analysis processing to describe the features within multiphase particles within minutes. This now provides opportunities for plant site–based 3-D coarse-particle characterization to be developed (Miller and Lin 2018).

PLANT-BASED OPERATIONS

Process diagnosis, flow-sheet design, and optimization are effectively and efficiently achieved through the use of metallurgical test work combined with modern quantitative mineralogical techniques (Lotter 2011; Gu et al. 2014). Several companies have applied the technology on a more routine basis to supply metallurgical operations with regular data. These have included Rio Tinto (KUCC concentrator), Barrick Gold Corporation, Freeport-McMoRan, Anglo American Platinum, and Glencore operations (formerly Xstrata and Falconbridge). The application of XRPD and XRF techniques have been extensively used over many years, in particular in areas such as the analysis of bauxites, fly ash, iron ore, sulfide mineralogy, and cement manufacturing.

Several case studies have been published that have demonstrated the effectiveness of incorporating automated mineralogy data for process improvements, particularly in optimizing grinding and flotation circuits (Baum et al. 2004; Dai et al. 2008; Rule and Schouwstra 2012; MacDonald et al.

2011; Lotter 2011; Lotter et al. 2010; examples in Becker et al. 2016).

Anglo Platinum was one of the pioneers in using automated SEM techniques to track the mineralogy of processing plants and ore sources (Schouwstra and Smit 2011). A detailed study into the losses of valuable minerals (PGMs and sulfides) using automated SEM techniques showed that an increase in the liberation of the valuable minerals was required to improve recoveries. Following piloting to demonstrate that finer grinding would increase the liberation and recovery of the valuable minerals, large-scale implementation was undertaken in 2009. The implementation yielded a 50% reduction in tailings grade with a corresponding increase in recovery of more than 5% of PGMs.

The most detailed evaluation incorporating all facets of analysis, including representative sampling routines, has been reported by Lotter and coworkers (Lotter 2011; Lotter et al. 2010). For example, the work illustrated for two case studies from Xstrata Nickel's (now part of Glencore) Nickel Rim South mine in Sudbury and its Raglan concentrator in Quebec, which incorporated the use of automated mineralogical techniques. A series of statistical benchmark surveys to describe the flow-sheet behavior under typical mining and milling conditions were conducted over many years (Lotter and Laplante 2007). At plant operations scale, a procedure was developed and validated whereby a representative suite of flow-sheet samples could be taken from an operating concentrator for mass and value balancing, followed by automated SEM (QEMSCAN) measurement across a series of closed size fractions. This work was used to update a concentrator's performance across several years and allowed for identifying opportunities for improving performance in the process.

CONCLUSIONS

Automated mineralogy methods, particularly automated SEM and XRPD systems, are now widely used for ore characterization, process design, and process optimization. These techniques deliver mineralogical information at fast acquisition times, can produce statistically representative analysis of a sample, as well as provide the ability to distinguish fine-grained or complexly intergrown minerals at the scale of micrometers. Several published case studies have demonstrated that large gains can be obtained through grinding and flotation optimization guided by automated mineralogy data. Improvements in both hardware and software will continue that will allow these techniques to be more versatile on mine sites and make them an essential tool for the metallurgist. The key factors that are important in using these automated techniques include

- Obtaining representative samples from the field and/or metallurgy process and suitably mounting them for analysis;
- Generating a mineral classification library and/or a suitable set of standards for analysis, which are representative of the mineral phases present in samples under examination;
- Establishing the limitations of analysis and what other complementary techniques can be used;
- Validating analytical results with other techniques; and
- Providing adequate training to staff.

For accurate mass balance derivations and deportment, assessments require quantitative compositional analyses from techniques such as EPMA and/or LA-ICPMS to validate mineral compositions. Emerging techniques, such as XCT, which allows measurement of materials in situ, will undoubtedly play an important role in the future.

REFERENCES

Amelinckx, S., van Dyck, D., van Landuyt, J., and van Tendeloo, G. 1997. *Electron Microscopy: Principles and Fundamentals*. Weinheim, Germany: VCH Wiley.

Anand, R.R., Gilkes, R.J., and Roach, G.I.D. 1989. Geochemical and mineralogical characteristics of bauxites, Darling Range, Western Australia. *Appl. Geochem*. 6(3):233–248.

Andersen, J.C.O., Rollinson, G.K., Snook, B., Herrington, R., and Fairhurst, R.J. 2009. Use of QEMSCAN for the characterization of Ni-rich and Ni-poor goethite in laterite ores. *Miner. Eng*. 22(13):1119–1129.

Armstrong, J.T. 1988. Quantitative analysis of silicates and oxide minerals: Comparison of Monte Carlo, ZAF and Phi-Rho-Z procedures. In *Microbeam Analysis*. Edited by D.E. Newbury. Berkeley, CA: San Francisco Press. pp. 239–246.

Aylmore, M.G., and Walker, G.S. 1998. Quantification of bauxites by the Rietveld method. *Powder Diffr.* 13(3):136–143.

Aylmore, M.G., Merigot, K., Quadira, Z., Rickard, W., Evans, N., McDonald, B., Catovic, E., and Spitalny, P. 2018a. Applications of advanced analytical and mass spectrometry techniques to the characterisation of micaceous lithium-bearing ores. *Miner. Eng.* 116:182–195.

Aylmore, M.G., Merigot, K., Rickard, W., Evans, N., McDonald, B., Catovic, E., and Spitalny, P. 2018b. Assessment of a spodumene ore by advanced analytical and mass spectrometry techniques to determine its amenability to processing for the extraction of lithium. *Miner. Eng.* 119:137–148.

Baum, W. 2014. Ore characterization, process mineralogy and lab automation a roadmap for future mining. *Miner. Eng.* 60:69–73.

Baum, W., Lotter, N.O., and Whittaker, P.J. 2004. Process mineralogy—a new generation for ore characterization and plant optimization. SME Preprint No. 04–12. Littleton, CO: SME. pp. 1–5.

Baumgartner, R., Dusci, M., Gressier, J., Trueman, A., Poos, S., Brittan, M., and Mayta, P. 2011. Building a geometallurgical model for early-stage project development—A case study from the Canahuire epithermal Au-Cu-Ag deposit, Southern Peru. In *First AusIMM International Geometallurgy Conference: Proceedings*. Edited by S. Dominy. Melbourne, Victoria: Australasian Institute of Mining and Metallurgy.

Baumgartner, R., Dusci, M., Trueman, A., Brittan, M., and Poos, S. 2013. Building a geometallurgical model for the Canahuire epithermal Au-Cu-Ag deposit, Southern Peru—past, present and future. In *Second AusIMM International Geometallurgy Conference: Proceedings*. Edited by S. Dominy. Melbourne, Victoria: Australasian Institute of Mining and Metallurgy.

Becker, M., Wightman, E.M., and Evans, C.L., eds. 2016. *Process Mineralogy*. Indooroopilly: Julius Kruttschnitt Mineral Research Centre, University of Queensland.

Best, E., Baum, W., Gilbert, R., Hohenstein, B., and Balt, A. 2007. The Phelps Dodge central analytical service center: Step change technology implementing robotics systems and lab automation in the copper industry. In *Proceedings of the Sixth International Copper–Cobre Conference*, Vol. 7. Montreal, QC: Canadian Institute of Mining, Metallurgy and Petroleum. pp. 119–126.

Bish, D.L., and Post, J.E., eds. 1989. *Reviews in Mineralogy*. Vol. 20, Modern Powder Diffraction. Edited by P.H. Ribbe. Chantilly, VA: Mineralogical Society of America.

Bish, D.L., and Post, J.E. 1993. Quantitative mineralogical analysis using the Rietveld full-pattern method. *Am. Mineral*. 78:932–940.

Bookin, A.S., Drits, V.A., Plancon, A., and Tchoubar, C. 1989. Stacking faults in kaolin-group minerals in the light of real structural features. *Clays Clay Miner*. 37(4):297–307.

Bouchet A., Proust, D., Meunier, A., and Beaufort, D. 1988. High-charge to low-charge smectites reaction in hydrothermal alteration processes. *Clays Clay Miner*. 23:133–146.

Bowell, R.J. Perkins, W.F., Tahija D., Ackerman, J., and Mansanti, J. 2005. Application of LA-ICPMS to trouble-shooting mineral processing problems at the Getchell mine, Nevada. *Miner. Eng.* 18:754–761.

Brindley, G.W. 1980. Quantitative x-ray mineral analysis of clays. In *Crystal Structures of Clay Minerals and Their X-Ray Identification*. Edited by G.W. Brindley and G. Broen. London: Mineralogical Society. pp. 411–438.

Buhrke, V.E., Jenkins, R., and Smith D.K., eds. 1997. *A Practical Guide for the Preparation of Specimens for X-Ray Fluorescence and X-Ray Diffraction Analysis*. New York: Wiley.

Bulled, D., 2007. Grinding circuit design for Adanac Moly Corp using a geometallurgical approach. In *Proceedings of the 39th Annual Canadian Mineral Processors Conference*. Edited by J. Folinsbee. Montreal, QC: Canadian Institute of Mining, Metallurgy and Petroleum.

Bulled, D., Leriche, T., Blake, M., Thompson, J., and Wilkie, T. 2009. Improved production forecasting through geometallurgical modelling at iron ore company of Canada. In *Proceedings of the 41st Annual Canadian Mineral Processors Conference*. Edited by R. Henderson. Montreal, QC: Canadian Institute of Mining, Metallurgy and Petroleum.

Cabri, L.J. 1981. Relationship of mineralogy for the recovery of PGE from ores. In *Platinum-Group Elements: Mineralogy, Geology, Recovery*, special vol. 23. Edited by L.J. Cabri. Montreal, QC: Canadian Institute of Mining, Metallurgy and Petroleum. pp. 233–250.

Cabri, L.J., Beattie, M., Rudashevsky, N.S., and Rudashevsky, V.N. 2005. Process mineralogy of Au, Pd and Pt ores from the Skaergaard Intrusion, Greenland, using new technology. *Miner. Eng.* 18:887–897.

Cabri, L.J., Rudashevsky, N.S., Rudashevsky, V.N., and Gorkovetz, V. 2008. Study of native gold from the Luopensulo deposit (Kostomuksha area, Karelia, Russia) using a combination of electric pulse disaggregation (EPD) and hydroseparation (HS). *Miner. Eng.* 21:463–470.

Cabri, L.J., Choi, Y., Nelson, M., Tubrett, M., and Sylvester, P.J. 2010. Advances in precious metal trace element analyses for deportment using LAM-ICP-MS. In *Proceedings of the 42nd Annual Canadian Mineral Processors Conference*. Edited by D. Fragomeni. Montreal, QC: Canadian Institute of Mining, Metallurgy and Petroleum. pp. 182–196.

Chryssoulis, S.L., and Cabri, L.J. 1990. Significance of gold mineralogical balance in mineral processing. *Trans. Inst. Min. Metall.*, Sect. C. 99:C1–C10.

Chryssoulis, S.L., and McMullen, J. 2016. Mineralogical investigation of gold ores. In *Gold Ore Processing: Project Development and Operations*, 2nd ed. Edited by M.D. Adams. Amsterdam: Elsevier. pp. 57–93.

Cnudde, V., and Boone, M.N. 2013. High-resolution X-ray computed tomography in geosciences: A review of the current technology and applications. *Earth Sci. Rev.* 123:1–17.

Cullity, B.D. 1978. *Elements of X-Ray Diffraction*, 2nd ed. Reading, MA: Addison-Wesley.

Dai, Z., Bos, J-A., Lee, A., and Wells, P. 2008. Mass balance and mineralogical analysis of flotation plant survey samples to improve plant metallurgy. *Miner. Eng.* 21:826–831.

Dobby, G., Bennett, C., Bulled, D., and Kosick, G. 2004. Geometallurgical modelling—the new approach to plant design and production forecasting/planning, and mine/mill optimization. In *Proceedings of the 36th Annual Canadian Mineral Processors Conference*. Montreal, QC: Canadian Institute of Mining, Metallurgy and Petroleum.

Dollase, W.A. 1986. Correction of intensities for preferred orientation in powder diffractometry: Application of the March model. *J. Appl. Crystallogr*. 19:267–272.

Evans, C.L., and Morrison, R.D. 2016. Mineral liberation. In *Process Mineralogy*. Edited by M. Becker, E.M. Wightman, and C.L. Evans. Indooroopilly: Julius Kruttschnitt Mineral Research Centre, University of Queensland. pp. 219–233.

Evans, C.L., and Napier-Munn, T.J. 2013. Estimating error in measurements of mineral grain size distribution. *Miner. Eng.* 52:198.

Evans, C.L., and Wightman, E.M. 2009. Modelling liberation of comminuted particles. SME Preprint No. 09-088. Littleton, CO: SME.

Fandrich, R., Gu, Y., Burrows, D., and Moeller, K. 2007. Modern SEM-based mineral liberation analysis. *Int. J. Miner. Process*. 84:310–320.

Fitzpatrick, R.W., and Schwertmann, U. 1982. Al-substituted goethite, an indicator of pedogenic and other weathering environments in South Africa. *Geoderma.* 27:335–347.

Fosu, S., Skinner, W., and Zanin, M. 2015. Detachment of coarse composite sphalerite particles from bubbles in flotation: Influence of xanthate collector type and concentration. *Miner. Eng.* 71:73–84.

Goldstein, J., Newbury, D., and Joy, D., eds. 2003. *Scanning Electron Microscopy and X-Ray Microanalysis.* New York: Springer. pp. 391–451.

Goodall, W.R. 2008. Characterisation of mineralogy and gold deportment for complex tailings deposits using QEMSCAN. *Miner. Eng.* 21:518–523.

Goodall, W.R., and Butcher, A.R. 2012. The use of QEMSCAN in practical gold deportment studies. *Miner. Process. Extr. Metall*. 121(4):199–204.

Goodall, W.R., Scales, P.J., and Butcher, A.R. 2005. The use of QEMSCAN and diagnostic leaching in the characterisation of visible gold in complex ores. *Miner. Eng.* 18:877–886.

Gottlieb, P., Argon-Olshina, N., and Sutherland, D.N. 1991. The characterisation of mineral matter in coal and fly ash. In *Proceedings of the Engineering Foundation Conference*. Edited by S.A. Benson. New York: American Society of Mechanical Engineers. pp. 135–145.

Gottlieb, P., Wilkie, G., Sutherland, D., Ho-Tun, E., Suthers, S., Perera, K., Jenkins, B., Spencer, S., Butcher, A.R., and Rayner, J. 2000. Using quantitative electron microscopy for process mineralogy applications. *JOM.* 52(4):24–25.

Gottlieb, P., Motl, D., Dosbaba, M., and Kopřiva, A. 2015. The use of the TIMA automated mineral analyzer for the characterization of ore deposits and optimization of process operations. Presented at the Austrian Mineralogical Society MinPet 2015.

Gu, Y. 2003. Automated scanning electron microscope based mineral liberation analysis. *J. Miner. Mater. Charact. Eng*. 2(1):33–41.

Gu, Y., Schouwstra, R.P., and Rule, C. 2014. The value of automated mineralogy. *Miner. Eng.* 58:100–103.

Harris D.C. 1998. *Quantitative Chemical Analysis*. New York: W.H. Freeman.

Hatton, D., and Hatfield, D. 2013. A geometallurgical approach to flotation process design using optimised grade-recovery curves. In *Proceedings of the 45th Annual Canadian Mineral Processors Conference*. Westmount, QC: Canadian Institute of Mining, Metallurgy and Petroleum. pp. 59–70.

Hem, S.R., de V. Louw, J.D., Gateshki, M., Göske, J., Rindbæk Larsen, O., and Strangeways, J. 2009. Sample preparation for quantitative Rietveld analysis, phase identification and XRF in one step: Automated sample preparation by Centaurus. In *Heavy Minerals Conference: "What Next?"* Symposium Series S57. Johannesburg: Southern African Institute of Mining and Metallurgy.

Henley, K.J. 1983. *Ore-Dressing Mineralogy: A Review of Techniques, Applications and Recent Developments*. Special Publication No. 7. Edited by J.P.R. De Villiers and P.A. Cawthorn. Johannesburg: Geological Society of South Africa. pp. 175–200.

Hill, R.J. 1991. Expanded use of the Rietveld method in studies of phase abundance in multiphase mixtures. *Powder Diffr.* 6:74–77.

Hill, R.J., and Howard, C.J. 1987. Quantitative phase analysis from neutron powder diffraction data using the Rietveld method. *J. Appl. Crystallogr*. 20:467–474.

Hill, R.J., and Madsen, I.C. 2002. Sample preparation, instrument selection and data collection. In *Structure Determination from Powder Diffraction Data*. Edited by W. David, K. Shankland, L. McCusker, and C. Baerlocher. New York: Oxford University Press. pp. 98–117.

Hill, R.J., Tsambourakis, G., and Madsen, I.C. 1993. Improved petrological modal analyses from X-ray powder diffraction data by use of the Rietveld method. Part I. Selected igneous, volcanic and metamorphic rocks. *J. Petrol*. 34:867–900.

Hoal, K.O., Woodhead, J., and Smith, K.S. 2013. The importance of mineralogical input into geometallurgy programs. In *Second AusIMM International Geometallurgy Conference: Proceedings*. Edited by S. Dominy. Melbourne, Victoria: Australasian Institute of Mining and Metallurgy.

Johnston, N.W. 2016. Sphalerite and galena liberation levels for the Mount Isa concentrator. In *Process Mineralogy*. Monograph Series in Mining and Mineral Processing, No. 6. Edited by M. Becker, E.M. Wightman, and C.L. Evans. Indooroopilly: Julius Kruttschnitt Mineral Research Centre, University of Queensland. pp. 234–249.

Klemd, R., and Bratz, H. 2016. Laser ablation ICP-MS. In *Process Mineralogy*. Edited by M. Becker, E.M. Wightman, and C.L. Evans. Indooroopilly: Julius Kruttschnitt Mineral Research Centre, University of Queensland. pp. 120–132.

Klug, H.P., and Alexander, L.E. 1974. *X-Ray Diffraction Procedures for Polycrystalline and Amorphous Materials*. New York: Wiley.

Kormos, L., Sliwinski, J., Oliveira, J., and Hill, G. 2013. Geometallurgical characterization and representative metallurgical sampling at Xstrata process support. In *Proceedings of the 45th Annual Canadian Mineral Processors*. Westmount, QC: Canadian Institute of Mining, Metallurgy and Petroleum.

Laplante, A.R., Woodcock, F., and Noaparast, M. 1995. Predicting gravity separation gold recovery. *Mineral. Metall. Process.* (May): 74–79.

Lastra, R., and Paktunc, D. 2016. An estimation of the variability in automated quantitative mineralogy measurements through inter-laboratory testing. *Miner. Eng.* 95:138–145.

Lastra, R., and Petruk, W. 2014. Mineralogical characterization of sieved and un-sieved samples. *J. Mineral. Mater. Charact. Eng*. 2(1):40–48.

Lastra, R., Price, J., Cabri, L.J., Rudashevsky, N.S., Rudashevsky, V.N., and McMahon, G. 2005. Gold characterization of a sample from Malartic East (Quebec) using concentration by hydroseparator. In *Proceedings of the International Symposium on the Treatment of Gold Ores*. Edited by G. Deschenes, D. Houdin, and L. Lorenzen. Montreal, QC: Canadian Institute of Mining, Metallurgy and Petroleum. pp. 17–29.

Li, D.Y., O'Connor, Roach, G.I.D., and Cornell, J.B. 1990. Use of x-ray powder diffraction pattern fitting: Characterising preferred orientation gibbsites. *Powder Diffr.* 5:79–85.

Li, J., McDonald, R.G., Kaksonen, A.H., Morris, C., Rea, S., Usher, K.M., Wylie, J., Hilario, F., and du Plessis, C.A. 2014. Applications of Rietveld-based QXRD analysis in mineral processing. *Powder Diffr.* 29(S1): 589–595.

Lin, C.L., Hsieh, C.H., Tserendagva, T.A., and Miller, J.D. 2013. Dual-energy rapid scan radiography for geometallurgy evaluation and isolation of trace mineral particles. *Miner. Eng.* 40:30–37.

Liu, Y., Gupta, R., Sharma, A., Wall, T., Butcher, A., Miller, G., Gottlieb, P., and French D. 2005. Mineral matter-organic matter association characterisation by QEMSCAN and applications in coal utilisation. *Fuel*. 84(10):1259–1267.

Longerich, H. 2008. Laser-ablation inductively coupled plasma-mass spectrometry (ICPMS). In *Laser-Ablation-ICPMS in the Earth: Current Practices and Outstanding Issues: Short Course*, Vol. 40. Edited by P. Sylvester. Vancouver, BC: Mineralogical Association of Canada.

Lotter, N.O. 1995. Review of evaluation models for the representative sampling of ore. *J. S. Afr. Inst. Min. Metall*. 95(4):149–155.

Lotter, N.O. 2011. Modern process mineralogy: An integrated multi-disciplined approach to flowsheeting. *Miner. Eng.* 24(12):1229–1237.

Lotter, N.O., and Laplante, A.R. 2007. Statistical benchmark surveying of production concentrators. *Miner. Eng.* 20:793–801.

Lotter, N.O., Di Feo, A., Kormos, L.J., Fragomeni, D., and Comeau, G. 2010. Design and measurement of small recovery gains: A case study at Raglan concentrator. *Miner. Eng.* 23:567–577.

Lotter, N.O., Oliveira, J.F., Hannaford, A.L., Amos, S.R., and Broughton, D.W. 2013. Flowsheet development for the hypogene geomet unit in the Ivanplats Kamoa copper project. In *Proceedings of the 45th Annual Canadian Mineral Processors Conference*. Westmount, QC: Canadian Institute of Mining, Metallurgy and Petroleum. pp. 71–85.

MacDonald, M., Adair, B.J.I., Bradshaw, D.J., Dunn, M., and Latti, D. 2011. Learnings from five years of on-site MLA at Kennecott Utah Copper Corporation. In *Proceedings of the 10th International Congress for Applied Mineralogy (ICAM)*. Heidelberg, Germany: Springer. pp. 419–426.

Madsen, I.C., and Hill, R. 1990. QPDA: User-friendly, interactive program for quantitative phase and crystal size/strain analysis of powder diffraction data. *Powder Diffr.* 5(4):195–199.

Madsen, I.C., and Hill, R. 1994. Collection and analysis of powder diffraction data with near-constant counting statistics. *J. Appl. Crystallogr.* 27(3):385–392.

Madsen, I.C., and Scarlett, N.V.Y. 1999. Cement: Quantitative phase analysis of portland cement clinker. In *Industrial Applications of X-ray Diffraction*. Edited by F.H. Chung and D.K. Smith. New York: Marcel Dekker. pp. 415–440.

Madsen, I.C., and Scarlett, N.V.Y. 2007. Quantitative phase analysis. In *Powder Diffraction: Theory and Practice*. Edited by R.E. Dinnebier and S.J.L. Billinge. London: Royal Society of Chemistry.

Madsen, I.C., Scarlett, N.V.Y., Cranswick, L.M.D., and Lwin, T. 2001. Outcomes of the International Union of Crystallography Commission on Powder Diffraction round robin on quantitative phase analysis: Samples 1*a* to 1*h*. *J. Appl. Crystallogr*. 34(Part 4):409–426.

Madsen, I.C., Scarlett, N.V.Y., and Whittington, B.I. 2005. Pressure acid leaching of nickel laterite ores: An in situ diffraction study of the mechanism and rate of reaction. *J. Appl. Crystallogr*. 38:927–933.

Madsen, I.C., Scarlett, N.V.Y., and Kern, A. 2011. Description and survey of methodologies for the determination of amorphous content via X-ray powder diffraction. *Z. Kristallogr.* 226(12):944–955.

Madsen, I.C., Scarlett, N.V.Y., Riley, D.P., and Raven, M.D. 2012. Quantitative phase analysis using the Rietveld method. In *Modern Diffraction Methods.* Edited by E.J. Mittemeijer and U. Welzel. Weinheim, Germany: Wiley-VCH.

Mariano, R.A., and Evans, C.L. 2015. Error analysis in ore particle composition distribution measurements. *Miner. Eng.* 82:36–44.

McCusker, L.B., Von Dreele, R.B., Cox, D.E., Louer, D., and Scardi, P. 1999. Rietveld refinement guidelines. *J. Appl. Crystallogr*. 32:36–50.

McIvor, R.E., and Finch, J.A. 1991. A guide to interfacing of plant grinding and flotation operations. *Miner. Eng.* 4(1):9–23.

McKay, N. 2016. Red Dog concentrator optimisation study 2009. In *Process Mineralogy*. Edited by M. Becker, E.M. Wightman, and C.L. Evans. Indooroopilly: Julius Kruttschnitt Mineral Research Centre, University of Queensland. pp. 250–260.

McKay, N., Wilson, S., and Lacouture, B. 2007. Ore characteristion of the Aqqaluk deposit at Red Dog. In *Proceedings of the 39th Annual Canadian Mineral Processors Conference.* Montreal, QC: Canadian Institute of Mining, Metallurgy and Petroleum. pp 55–74.

Miller, J.D., and Lin, C.L. 2018. X-ray tomography for mineral processing technology—3D particle characterization from mine to mill. *Miner. Metall. Process.* 35(1):1–12.

Montoya, P.A., Keeney, L., Jahoda, R., Hunt, J., Berry, R., Drews, U., Chamberlain, V., and Leichliter, S. 2011. Geometallurgical modelling techniques applicable to prefeasibility projects–La Colosa case study. In *First AusImm International Geometallurgy Conference: Proceedings*. Edited by S. Dominy. Melbourne, Victoria: Australasian Institute of Mining and Metallurgy.

Mosser-Ruck, R., Devineau, K., Charpentier, D., and Cathelineau, M. 2005. Effects of ethylene glycol saturation protocols on XRD patterns: A critical review and discussion. *Clays Clay Miner.* 53(6):631–638.

Napier-Munn, T.J. 2014. *Statistical Methods for Mineral Engineers: How to Design Experiments and Analyse Data*. Indooroopilly: Julius Kruttschnitt Mineral Research Centre, University of Queensland.

Neder, R.B., Burghammer, M., Grasl, T.H., Schulz, J.H., Bram, A., and Fiedler S. 1999. Refinement of the kaolinite structure from single-crystal synchrotron data. *Clays Clay Miner*. 47(4):487–494.

Norrish, K., and Hutton, J.T. 1969. An accurate x-ray spectrographic method for the analysis of a wide range of geological samples. *Geochim. Cosmochim. Acta.* 431:33.

O'Brien, G., Gu, Y., Adair, B., and Firth, B. 2011. The use of optical reflected light and SEM imaging systems to provide quantitative coal characterisation. *Miner. Eng.* 24:1299–1304.

O'Connor, B.H., Li, D.Y., and Sitepu, H. 1991. Strategies for preferred orientation corrections in x-ray powder diffraction using line intensity ratios. *Adv. X-ray Anal*. 34:1–7.

Petruk, W. 1976. The application of quantitative mineralogical analysis of ores to ore dressing. *CIM Bull.* 767:146–153.

Petruk, W. 2000. *Applied Mineralogy in the Mining Industry*. Amsterdam: Elsevier.

Petruk, W., and Hughson, M.R. 1977. Image analysis evaluation of the effect of grinding media on selective flotation of two zinc–lead–copper ores. *CIM Bull.* 787:128–135.

Petruk, W., and Schnarr, J.R. 1981. An evaluation of the recovery of free and unliberated mineral grains, metals and trace elements in the concentrator of Brunswick Mining and Smelting Corporation Limited. *CIM Bull.* 833:132–159.

Pirard, E. 2016. Optical microscopy. In *Process Mineralogy*. Edited by M. Becker, E.M. Wightman, and C.L. Evans. Indooroopilly: Julius Kruttschnitt Mineral Research Centre, University of Queensland. pp. 51–66.

Pouchou J.L., and Pichoir F. 1985. "PAP," procedure for improved quantitative microanalysis. In *Microbeam Analysis*. Edited by J.T. Armstrong. Berkeley, CA: San Francisco Press. pp. 104–106.

Pownceby, M.I., and MacRae, C.M. 2016. Electron probe microanalyser. In *Process Mineralogy*. Edited by M. Becker, E.M. Wightman, and C.L. Evans. Indooroopilly: Julius Kruttschnitt Mineral Research Centre, University of Queensland. pp. 79–96.

Rietveld, H.M. 1969. A profile refinement method for nuclear and magnetic structures. *J. Appl. Crystallogr*. 2(2):65–71.

Rousseau, R.M. 2006 Corrections for matrix effects in X-ray fluorescence analysis—a tutorial. *Spectrochim. Acta, Part B*. 61:759–777.

Rule C., and Schouwstra, R.P. 2012. Process mineralogy delivering significant value at Anglo Platinum concentrator operations. In *Proceedings of the 10th International Congress for Applied Mineralogy (ICAM)*. Edited by M. Broekmans. Berlin: Springer.

Scarlett, N.V.Y., and Madsen, I.C. 2006. Quantification of phases with partial or no known crystal structures. *Powder Diffr.* 21(4):278–284.

Scarlett, N.V.Y., Madsen, I.C., Manias, C., and Retallack, D. 2001. On-line x-ray diffraction for quantitative phase analysis: Application in the portland cement industry. *Powder Diffr.* 16:71–80.

Scarlett, N.V.Y., Madsen, I.C., Cranswick, L.M.D., Lwin, T., Groleau, E., Stephenson, G., Aylmore, M., and Agron-Olshina, N. 2002. Outcomes of the International Union of Crystallography Commission on powder diffraction round robin on quantitative phase analysis: Samples 2, 3, 4, synthetic bauxite, natural granodiorite and pharmaceuticals. *J. Appl. Crystallogr*. 35:383–400.

Scarlett, N.V.Y., Madsen, I.C., and Whittington, B.I. 2008. Time-resolved diffraction studies into the pressure acid leaching of nickel laterite ores: a comparison of laboratory and synchrotron X-ray experiments. *J. Appl. Crystallogr.* 41: 572-583.

Schouwstra, R.P., and Smit, A.J. 2011. Developments in mineralogical techniques—What about mineralogists? *Miner. Eng.* 24(12):1224–1228.

Schulze, D.G. 1984. The influence of aluminum on iron oxides. VIII. Unit cell dimensions of Al-substituted goethites and estimation of Al from them. *Clays Clay Miner.* 32:36–44.

Smythe, D.M., Lombard, A., and Coetzee, L.L. 2013. Rare earth element deportment studies utilising QEMSCAN technology. *Miner. Eng.* 52:52–61.

Snyder, R.L., and Bish, D.L. 1989. Quantitative analysis. In *Reviews in Mineralogy*. Vol. 20, Modern Powder Diffraction. Edited by P.H. Ribbe. Chantilly, VA: Mineralogical Society of America. pp. 101–144.

Spencer, S., and Sutherland, D. 2000. Stereological correction of mineral liberation grade distributions estimated by single sectioning of particles. *Image Anal. Stereology* 19:175–182.

Sutherland, D. 2007. Estimation of mineral grain size using automated mineralogy. *Miner. Eng.* 20:452–460.

Taylor, J.C., and Matulis, C.E. 1991. Absorption contrast effects in the quantitative XRD analysis of powders by full multiphase profile refinement. *J. Appl. Crystallogr.* 24:14–17.

Taylor, J.C., and Rui, Z. 1992. Simultaneous use of observed and calculated standard profiles in quantitative XRD analysis of minerals by the multiphase Rietveld method: The determination of pseudorutile in mineral sands products. *Powder Diffr.* 7:152–161.

Tsikouras, V., Pe-Piper, G., Piper, D.J.W., and Shaffer, M. 2011. Varietal heavy mineral analysis of sediment provenance, Lower Cretaceous Scotian Basin, eastern Canada. *Sediment. Geol.* 237:150–165.

Van Alphen, C. 2007. Automated mineralogical analysis of coal and ash products: Challenges and requirements. *Miner. Eng*. 20:496–505.

Walenta, G., and Füllmann, T. 2004. Advances in quantitative XRD analysis for clinker, cements, and cementitious additions. *Powder Diffr*. 19:40–44.

Wang D., Yuan X., Gu Y., Case T., Feser M., and Schouwstra R.P. 2014. Investigation of microCT (computed tomography) for 3-dimensional mineral characterization: A dual energy approach. In *Third International Symposium on Process Mineralogy (Process Mineralogy '14)*. Cornwall, UK: Minerals Engineering International.

Whittington, B.I., Johnson, J.A., Quan, L.P., McDonald, R.G., and Muir, D.M. 2003. Pressure acid leaching of arid-region nickel laterite ore. Part II. Effect of ore type. *Hydrometallurgy.* 70:47–62.

Wightman, E.M., Evans, C.L., Becker, M., and Gu, Y. 2016. Automated scanning electron microscopy with energy dispersive spectrometry. In *Process Mineralogy*. Edited by M. Becker, E.M. Wightman, and C.L. Evans. Indooroopilly: Julius Kruttschnitt Mineral Research Centre, University of Queensland. pp. 97–107.

Williams, S., and Richardson, J. 2004. Geometallurgical mapping: A new approach that reduces technical risk. In *Proceedings of the 36th Annual Canadian Mineral Processors Conference*. Montreal, QC: Canadian Institute of Mining, Metallurgy and Petroleum.

Young, R.A., ed. 1995. *The Rietveld Method*. Vol. 5, International Union of Crystallography Monographs on Crystallography. New York: Oxford University Press.

Zevin L.S., Kimmel, G., and Mureinik, I. 1995. *Quantitative X-Ray Diffractometry*. New York: Springer.

Zhou, J., and Gu, Y. 2016. Geometallurgical characterization and automated mineralogy of gold ores. In *Gold Ore Processing: Project Development and Operations*, 2nd ed. Edited by M.D. Adams. Amsterdam: Elsevier. pp. 95–111.

Zhou, J.Y., and Cabri, L.J. 2004. Gold process mineralogy: Objectives, techniques and applications. *J. Miner. Met. Mater. Soc.* 56(7):49–52.